New frontiers in nuclear physics with high-power lasers and brilliant monochromatic gamma beams

2016 Phys. Scr. 91 093004

(http://iopscience.iop.org/1402-4896/91/9/093004)

IOP Publishing | Royal Swedish Academy of Sciences Physica Scripta

Phys. Scr. **91** (2016) 093004 (23pp) doi:10.1088/0031-8949/91/9/093004

Invited Comment

New frontiers in nuclear physics with high-power lasers and brilliant monochromatic gamma beams

S Gales, D L Balabanski, F Negoita, O Tesileanu, C A Ur, D Ursescu and N V Zamfir

Extreme Light Infrastructure—Nuclear Physics (ELI-NP), Horia Hulubei National Institute for R&D in Physics and Nuclear Engineering (IFIN-HH), 30 Reactorului Str., 077125 Magurele, jud. Ilfov, Romania

E-mail: sydney.gales@eli-np.ro

Received 25 March 2016, revised 23 June 2016
Accepted for publication 4 July 2016
Published 8 August 2016

Abstract

The development of high power lasers and the combination of such novel devices with accelerator technology has enlarged the science reach of many research fields, in particular particle and nuclear physics, astrophysics as well as societal applications in material science, nuclear energy and applications for medicine. The European Strategic Forum for Research Infrastructures has selected a proposal based on these new premises called the Extreme Light Infrastructure (ELI). The ELI will be built as a network of three complementary pillars at the frontier of laser technologies. The ELI-NP pillar (NP for nuclear physics) is under construction near Bucharest (Romania) and will develop a scientific program using two 10 PW lasers and a Compton back-scattering high-brilliance and intense low-energy gamma beam, a combination of laser and accelerator technology at the frontier of knowledge. This unique combination of beams that are unique worldwide allows us to develop an experimental program in nuclear physics at the frontiers of present-day knowledge as well as society driven applications. In the present paper, the technical description of the facility as well as the new perspectives in nuclear structure, nuclear reactions and nuclear astrophysics will be presented.

Keywords: high power laser, high brilliance gamma beams, laser driven nuclear physics, nuclear and astrophysics, applications

(Some figures may appear in colour only in the online journal)

1. Introduction

Ultra-intense laser fields, reaching up to 10^{22} W cm^{-2}, are now able to produce typical radiation formerly used in nuclear facilities, as demonstrated in laboratories across the globe. The emerging laser driven technologies are very promising in terms of cost, size and their available parameter range. However, the vast majority of the experiments were performed in laboratories where the operation of the laser system does not reach the reliability of their nuclear facilities counterparts. Crossing the gap from lab-based experiments to facility-based experiments was identified, in Europe, as a major step forward. As a consequence, the construction of a state of the art laser-centred, distributed pan-European research infrastructure, involving ultrashort and ultra-intense laser technologies, was initiated through the Extreme Light Infrastructure (ELI) project. In 2006 the European Strategic Forum for Research Infrastructures (ESFRI) selected a proposal based on ultra-intense laser fields with intensities reaching up to $10^{22\text{-}23}$ W/cm^2 called 'ELI'. The construction of the research infrastructure, received the approval for funding in 2011-2012.

The three pillars of the ELI facility are being built in the Czech Republic, Hungary and Romania [1]. The Romanian pillar is the ELI-nuclear physics (ELI-NP) [2]. The new facility is intended to serve a broad national European and International science community. Its mission covers scientific research at the frontier of knowledge involving two domains. The first one is laser-driven experiments related to nuclear physics, strong-field quantum electrodynamics and associated vacuum effects. The second is based on a Compton—back-scattering high-brilliance and intense low-energy gamma beam (<20 MeV), a combination of laser and accelerator technology which will allow us to investigate nuclear structure and reactions as well as nuclear astrophysics with unprecedented resolution and accuracy [3–7]. In addition to fundamental themes, a large number of applications with significant societal impacts are being developed. These applications extend from nuclear power plant waste management to new radio-isotopes for medicine and cancer therapy and from space science to material and nanoscience using, for example, new powerful probes like a brilliant positron beam [8–10].

The ELI-NP research centre will be located in Magurele near Bucharest, Romania. The facility, worth more than 310 million euros, is supported financially by the European Regional Development Fund in two phases: 134 million euros in 2013-2015 and the rest in the 2014-2020 cycle of the European Funds. The project is implemented by Horia Hulubei National Institute for Physics and Nuclear Engineering (IFIN-HH). The project started in January 2013 and the new facility will be operational by the end of 2018. The civil engineering construction has started in June 2013 and should be completed by the spring of 2016.

During the last three years, a significant fraction of the international scientific community contributed to the shaping of the ELI-NP facility science program through a series of international workshops. As a result, these scientific meetings led to the definition of around ten new development directions for the experiments to be carried out at the future facility. For each of them, the writing of Technical Design Reports (TDRs) by specialized working groups of international scientists and coordinated by ELI-NP physics team, was triggered and further developed during the workshops. A final version of the TDR's were presented and discussed by the ELI-NP International Scientific Advisory Board in June 2015 [11].

In the following paper, we will present the new research areas at reach and/or to be revisited using the unique features of High Power Laser System (HPLS) up to 2 × 10 PW and of the brilliant and monochromatic Gamma Beam System (GBS) with energy 0.2-20 MeV. We will describe first the HPLS and the impact of this new probe on nuclear physics. Laser driven nuclear physics encompasses electron and ion acceleration with the promise of solid state density bunches for fusion-fission reactions to produce very neutron rich nuclei relevant for astrophysics. Nuclear reaction rates and isomer production in laser plasma and a very high flux of neutrons will be also investigated. In the second part of this paper, we will present the characteristics of the nearly completely polarized, intense and quasi-monochromatic gamma beam (from 0.2 to 20 MeV) of the ELI-NP facility. We will then discuss the perspectives of photonuclear reactions with this unique probe in the following fields:

- The study of electromagnetic dipole responses of atomic nuclei with real photon beams.
- Nuclear resonance fluorescence experiments mainly in uncovered areas of the nuclear chart.
- Nuclear collective excitation modes (Giant and Pygmy resonances) and the competition between various decay channels.
- Unique (γ, n), (γ, p) and (γ, α) measurements for p-process and nucleosynthesis.
- Photo-fission studies: rare fission modes, ternary fission.
- The separation and manipulation of neutron-rich isotopes via the construction of an ELI-NP IGISOL facility for nuclear structure studies of refractory elements.
- Applications of high brilliance gamma beams in nuclear energy, industry and medicine.

2. Laser driven Nuclear physics

2.1. A description of the high power laser system and laser beam delivery

The charged particle accelerators drove forward the progress of nuclear physics, material science and related applications in the past century. They offer a broad range of ionizing radiation combined with directionality and full control of the radiation parameters. They are based on electromagnetic fields that control the acceleration, steering and ability to focus the charged particles. The electric fields involved in the process are generated in capacitor or cavity systems reaching up to tens of MV/m, limited by electric breakdown process in vacuum. Hence, accelerating particles to GeV range requires hundreds of meter or even kilometers of acceleration structures.

An alternative path to particle acceleration is hence related to the production of electric fields beyond the limit in reach at the radiofrequency ranges and below. This can be achieved with the use of the laser pulses in vacuum and in plasmas. The maximum electric field in a laser pulse is determined by the laser intensity only and is given by the relation:

$$E_{\max}\left[\left(\frac{V}{cm}\right)\right] \cong 2.75 \times 10^{9}\left(\frac{I_L}{10^{16}\ \mathrm{W/cm^2}}\right)^{1/2} \qquad (1)$$

While the highest intensity reported to date is in the range of 10^{22} W/cm^2 [12], the electric fields generated in this way enter in the range of TV/cm. These huge fields could dramatically reduce the length of the particle accelerators. Unfortunately, the Lawson-Woodward theorem states that no net energy gain results for a relativistic electron interacting with the laser fields over an infinite interaction distance when reasonable assumptions about the interactions are made [13, 14].

The alternative approach is to use a plasma medium as support for a generation of transient electric fields based on the ponderomotive force of the electromagnetic field. In this case, the electric field resulting from the interaction is described by the following formula:

$$E\,(V/\mathrm{cm}) \approx 1.0 \times 10^{7}\left(\frac{I_L}{10^{16}\ \mathrm{W/cm^2}}\right) \times \left(\frac{10^{21}\ \mathrm{cm^{-3}}}{n_{ec}}\right)\left(\frac{100\mu\mathrm{m}}{r_L}\right) \quad (2)$$

Where n_{ec} is the electron critical density, r_L is the laser spot radius [15]. The electric fields generated in the plasma increase faster with the laser intensity than the electric field of the laser pulse itself. The critical density of the electrons is determined by the laser wavelength only and it is in the range of a few times 10^{21} $\mathrm{cm^{-3}}$ for laser frequency in the visible range. Reducing the spot size and boosting intensity of the laser to 10^{20} $\mathrm{W/cm^2}$ brings the ponderomotive field values close to the laser field values. The ponderomotive field and the laser field above can be used as fast evaluation of the generated fields. In practice, significant efforts are put in finding solutions to produce higher fields. This is possible by laser developments that allow higher intensities.

The laser system at the core of the ELI-NP facility was specified by the ELI-NP team with the support of the international community as a balance between the needs of the community and the realistic expectations on the existing state of the art technology. Based on the chirped pulse amplification scheme (CPA) [16], the high power laser system (HPLS) shall deliver peak power in the range of 10 PW, in pulses of the order of 20 fs on each of the two parallel amplification chains.

Further outputs of the HPLS were included in the design in addition to the two main outputs at 10 PW level, in order to optimize the use of the laser system as a facility with minimal downtime for maintenance. As a consequence, two optical compressors at the 100 TW level were included in the HPLS to allow test experiments running at a repetition rate of 10 Hz, while two further optical compressors were designed for the 1 PW level outputs running at 1 Hz. These outputs are useful in particular in the specific configurations where the experiments are not very demanding in high peak power but in average energy delivered on the target.

The front end is one of the most complex and sensitive parts of the CPA amplification chain and often requires maintenance and tweaking. In order to further reduce the downtime of the facility, HPLS will have a dual front end, operating only one at a time.

The HPLS has to deliver pulses in several experimental areas, marked, for convenience as E1, E4, E5, E6, E7. The E1 experimental area was designed to accommodate two 10 PW laser pulses focused on targets using short focal distance parabolic mirrors, for performing experiments related to nuclear physics. The E4 area will accommodate simultaneously two 100 TW beams for experiments related to gamma-gamma scattering and further parasitic beam time experiments. E5 will have both 1 PW outputs synchronous in the interaction chamber where secondary radiation sources shall be developed for the applicative part of the research at ELI-NP. The E6 area will accommodate two 10 PW pulses of the HPLS, one of them focused with a long focal distance parabolic mirror. The E7 experimental area shall also accommodate the two 10 PW outputs, having in addition as a exquisite feature the synchronous gamma beam from the GBS facility in ELI-NP. Figure 1 displays the sketch of the HPLS and delivery pulse characteristics to the experimental areas.

As pointed out, the key parameter for reaching extreme fields with the laser is the laser intensity I. It depends on the energy of the pulse E, on pulse duration τ and on spot size σ as follows: $I = E/\tau\sigma$. With an energy per pulse E of about 200 J and pulse duration τ of 20 fs, the peak power of the laser pulse reaches 10 PW, several times larger than any other existing laser system. With a spot size σ of 10 $\mu\mathrm{m}^2$ we can obtain intensities in the range of 10^{23} $\mathrm{W/cm^2}$.

The extracted energy is limited by the size and quality of the amplification crystals. The HPLS design targets a useful aperture of Ti:Sapphire crystals of 20 cm diameter while the largest one demonstrated to date is about 17 cm in diameter. No laser system with these parameters exists to date, HPLS intends to be the first running facility with these parameters. Pulse repetition rate for the 10 PW outputs shall be at the level of one shot per minute, limited by the repetition rate of the pump lasers of the HPLS Ti:Sapphire final amplifiers. The intermediate amplifiers will use higher repetition rate pump lasers, allowing 10 Hz repetition rate at parasitic outputs of 100 TW peak power, and of 1 Hz at outputs delivering 1 PW peak power.

Beam pointing stability is a key ingredient of the reproducible experiments, in particular when mass limited targets are involved. Such targets have dimensions similar to the spot size, in the range of a few micrometers, and the good pointing stability makes it possible to hit such targets in single shot experiments. Beam polarization state is determined by the orientation of the optical gratings in the optical compressors. The polarization state is linear. The polarization is horizontal, relative to the surface of the Earth. The high temporal contrast is one more essential ingredient for performing clean experiments. This parameter indicates how much light arrives at various delays before the main pulse reaches the target used in experiment. The temporal contrast is expressed as the ratio of the peak intensity to the intensity of the field at a given moment in time. The reference value for the HPLS are 10^{12}:1 at 100 ps in advance of the main pulse. The use of optical parametric amplification and cross polarized wave systems in the HPLS amplification chains shall make such values possible. But even at this good contrast level, the energy pedestal for a 10^{23} $\mathrm{W/cm^2}$ is reaching 10^{11} $\mathrm{W/cm^2}$, enough to produce a plasma plume that can be detrimental to the experiment. The measurement of such large temporal contrast values remains a challenge while the best device on the market only reaches 10^{11}:1 dynamic range.

The energy stability shall be better than 2% over 100 shots rms, in order to perform systematic reproducible studies. This stability is possible with the help of pump lasers, one of the challenges of the HPLS project. In order to

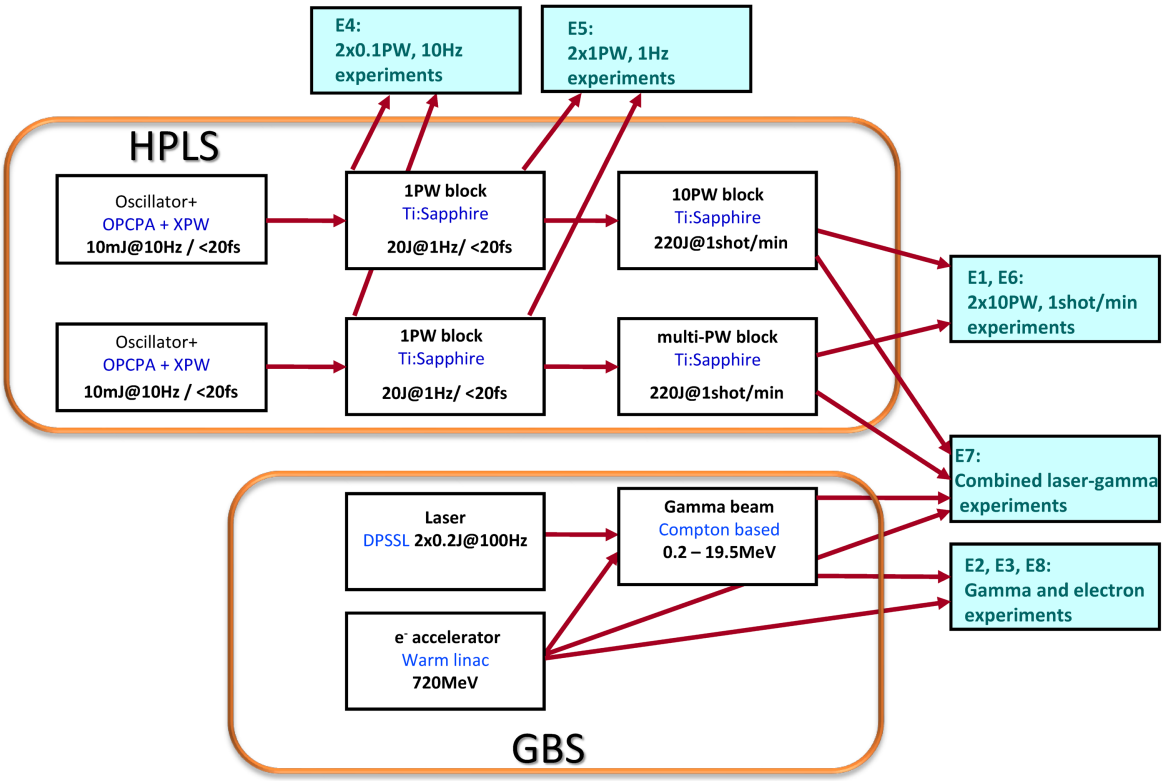

Figure 1. Sketch of the ELI-NP facility that includes the HPLS and GBS main devices and the experimental areas denoted E1, E2,… E8.

distribute the laser pulses to all the experimental areas, as mentioned above, extensive work was performed to design a distribution system for the laser outputs. The distribution system has to preserve the quality of the laser pulses and shall also control and further enhance specific laser pulses parameters. For the beam transport systems from the two 10 PW outputs to the experimental areas E1, E6 and E7, an optical system to transform the linear in circular polarization was considered, together with plasma mirrors that further improves the temporal contrast of the pulses on time scales below 30 ps. Based on the international scientific community requests for the ELI-NP facility, a number of features are now under consideration, like probe beam capability to produce plasma with high temperature and ionization degree to be used as target in some experiments and a timing system for the facility distributed to all experimental areas with ns or even fs resolution in order to provide triggering signals for all the detectors and diagnostics.

The diagnostics of the pulses close to the target is an important issue to be solved. While pulse duration can be obtained after compressor, the pointing stability and wave front analysis in the interaction chamber is essential for experiments. The HPLS will have built-in diagnostics for all six outputs. Last but not least, laser beam dumps, shutters, energy attenuation control shall be implemented in HPLS.

The number of shots to be delivered at each experimental area is limited by the radioactivity source terms and subsequent activation and cooling time. The layout of the experimental area in the ELI-NP facility is depicted in figure 2. It is placed between the HPLS room and GBS room and has eight experimental zones, denoted with E1, E2, ...E8. Specific experimental program was proposed for each of these areas, taking into account the specific parameters of the GBS or HPLS beams delivered and subsequent source terms associated with them.

2.2. Laser driven nuclear physics experiments

Recently, the huge development of the high power laser systems allows for a wide range of applications related to both, fundamental and applied physics research. In the nuclear physics field, the advantages brought by lasers are extremely important for several promising new experimental methods. For example, the interaction of high power lasers at an intensity greater than 10^{18} W/cm^2 with solid targets, could release accelerated ions with MeV range energies, which further, can be used for inducing nuclear reactions in secondary targets. The energy of the laser-accelerated particles depend on a multitude of factors, notably the laser intensity and the target parameters, driving the acceleration mechanism.

The powerful lasers of ELI-NP will reach intensities in the 10^{23} W/cm^2 regime, never obtained up until now, allowing full exploration of the radiation pressure acceleration (RPA) mechanism [17, 18]. With respect to the 'traditional' target normal sheath acceleration (TNSA) mechanism [19], RPA promises key features, such as quasi monoenergetic distribution, high bunch density and more efficiency in the acceleration resulting in a predicted increase of the beam energy. Indeed, if the ion acceleration is done in TNSA by the

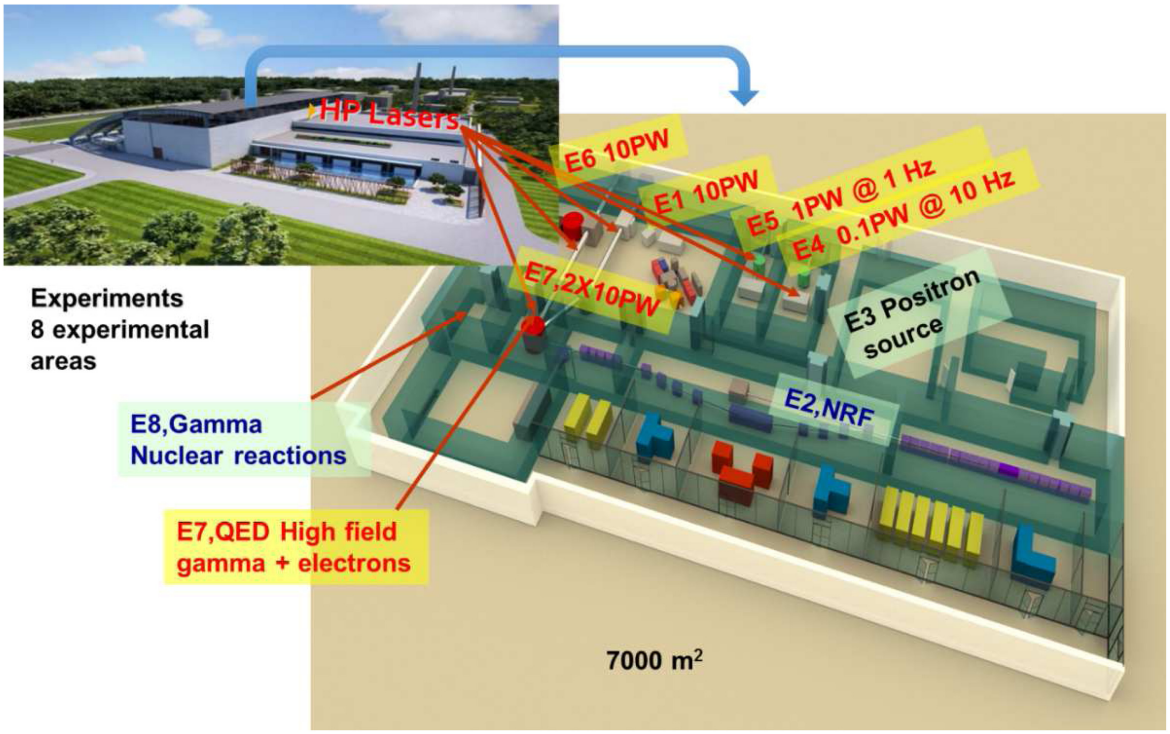

Figure 2. 3D sketch of the layout of the experimental areas.

electrostatic potential created by the electron cloud pushed out on the rear side of the target by the laser interaction, the use of very thin (nanometric scale) targets and circularly polarized beams with high contrast, produces in RPA a cold electron compression in front of the laser pulse which accelerate the ions via the created dipole Coulomb field. This difference in the acceleration mechanism allows a linear scaling of the ion energy with the laser intensity in the case of RPA, versus only a square root scaling in the case of TNSA. Moreover, the 'light sail' regime of RPA is expected to provide quasi-neutral and quasi-monoenergetic ion bunches with solid state density ($\sim 10^{22}$ atoms/cm^3), many orders of magnitude more dense than the ion bunches provided by 'classical' accelerators ($\sim 10^{8}$ atoms/cm^3). Achieving such a high quality beam is not only important *per se* but also for a multitude of experiments, such as the exploration of the neutron rich region of the r-process path with the fission-fusion scenario [20].

The targeted N ~ 126 region is of maximal importance for understanding the nucleosynthesis of heavy elements since it represents a waiting point of the r-process path. The details of the proposed exotic nuclei production scheme are given elsewhere [20], here we retain the basic principle of laser accelerated Th nuclei fissioning in flight and impinging a secondary Th fission target, the high bunch density increasing to probability for fusion of two low mass fission fragments, producing the nuclei of interest.

The production cross-section for such n-rich nuclei drops dramatically, making them inaccessible even for future 'conventional' radioactive beam facilities such as FAIR [21] or SPIRAL II [22]. Consequently, the laser-based acceleration technology could play a major role, producing bunches of accelerated ions with solid-state-like density in order to compensate this tiny production probability.

A plasma environment is expected to produce changes also in other nuclear observable: decay modes and half-life of unstable states as a result of the interaction of the nuclei with the photon and electron flux, but also due to changes in the electron cloud around nuclei, i.e. ionizing state. The plasma conditions created at ELI-NP by high power lasers could reveal various nuclear excitation and de-excitation mechanisms, some of them predicted but never observed up to now. Among the exotic processes which could occur in hot and dense plasma conditions are the nuclear excitation/de-excitation mechanisms involving the bound states of the electronic cloud. For example a nuclear excitation could occur following an electron capture from continuum, so-called nuclear excitation by electron capture (NEEC) process or following an electronic transition de-excitation in the nuclear excitation by electronic transition (NEET) process. Reversely, a nuclear de-excitation could have as consequence the emission of a bound electron to the continuum (IC—internal conversion process) or to another bound state (BIC—bound internal conversion process).

NEEC has never been observed up to now, while NEET has been measured only in cold targets [23–25], never in plasma conditions. Unstable nuclei ^{93}Mo [26] and ^{84}Rb [27] are among the best candidates to observe these processes, both having a long lifetime isomer and a nanosecond isomer at few keV higher excitation energy. These processes will be studied at ELI-NP in experiments which involves two laser beams. One laser beam accelerates ions from a primary target,

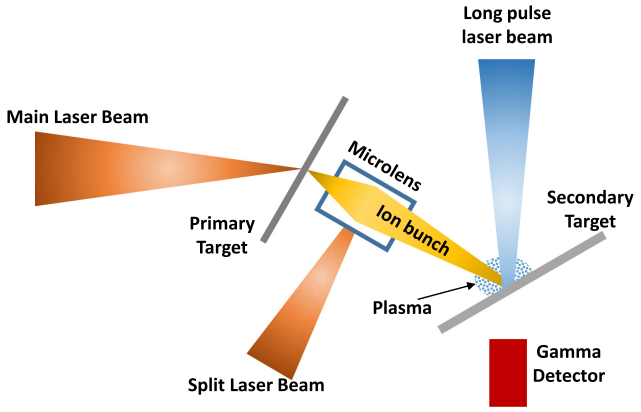

Figure 3. Schematic experimental configuration to study nuclear excitations in laser induced plasma.

producing isomeric states of interest, and a second one (with nanosecond duration) will create the required plasma conditions. In this way, the nucleus is excited to upper states which could decay much faster to the ground state, with a direct consequence on the apparent lifetime of the isomeric state under study. Similar to the research dedicated to the electron screening effect described previously, the experimental requirements in this case are mainly a high flux of accelerated particles and moderate energies in order to produce the largest possible number of nuclear reactions and states under study, rather than a high energy of the accelerated particles. The experimental setup for such an experiment is shown schematically in figure 3. We note that plasma production requires laser intensities of 10^{15}–10^{16} W cm^{-2} which means a laser spot size of about 100 μm diameter for ELI-NP laser pulses amplified to about 300 J and about 1 ns duration. If divergence of the primary ion beam is too large to match such spot on the secondary target, a microlens [28] triggered by a delayed laser split can be employed for ion collimation.

As studied processes occur at rather high plasma temperatures and densities, conditions established only in a small volume during the secondary target irradiation with the nanosecond duration laser pulse, another option to enhance the number of transitions of interest is the plasma trapping using high B-fields generation devices such as proposed by Moustaizis *et al* [29] which can reach up to 100 T over a cm^3 volume and for a microsecond duration. On the other hand, the detection part of the experimental setup has to be able to measure low energy gamma rays generated by the short lived nuclear state, as soon as possible after the production inside laser plasma [27]. Gamma detector systems able to fulfil this requirement are under development at ELI-NP.

The ability to produce very hot and dense plasma conditions at ELI-NP, could help in understanding the processes involving unstable nuclei in explosive stellar environments. In particular, the study of ^{26}Al isotope could have a wide range of consequences for astrophysical nuclear research. More precisely, the measurement of the effective lifetime of the ^{26}Al state is extremely important since its decay provides evidence for the ongoing galactic nucleosynthesis. Theoretical estimations [30] of this lifetime predict a dramatic decrease with a factor of 10^9 for high temperatures 0.15 to 0.4 GK as consequence of excitation of higher states and the presence of a beta decaying isomeric state of much shorter lifetime than the ground state. The estimation of different mechanisms which contribute to this decrement in hot plasma conditions is included in the physics program of ELI-NP.

As mentioned previously, the applications of the high power lasers are not restrained to fundamental physics, but will cover wide areas of applied physics research. In the following we would like to discuss the opportunities provided at ELI-NP for developing laser based sources of neutrons and muons in relation with laser-driven nuclear physics program. The impact of such sources spreads over multiple research areas from material science, biology and nuclear physics. Only for the latter case, neutron sources are widely used in multitude of directions such as nuclear waste transmutation, tests of the sensitive material for nonproliferation purposes, etc. High power lasers could generate very brilliant neutron bunches with short time duration via interactions of laser accelerated protons or deuterons with solid targets. A recent experiment at 200 TW Trident facility [31] revealed neutron energies above 10 MeV at 5×10^9 n/sr. In this case, the excellent laser contrast and intensity (10^{20}–10^{21} W cm^{-2}) allowed the proton acceleration via BOA (Break Out Afterburner) mechanism [32] on 400 nm deuterated plastic foils. A preliminary estimation [33] predicts a yield of about 10^{11} n/sr per laser shot achievable at ELI-NP.

The neutrons could be also generated in photonuclear reactions, i.e. by interaction of energetic gamma rays. In this case, the gammas are produced by laser accelerated electrons on high-Z targets. In an experiment [34] at Texas Petawatt Laser facility [35] a neutron flux of 10^{18} n cm^{-2} s has been obtained in a time interval smaller than 50 ps. Such characteristics of the neutrons source could be exploited optimally by fast neutron resonance radiography (FNRR) [36] for the non-intrusive identification of different types of materials, notably special nuclear materials, explosives, etc. The method is based on element specific absorption of neutrons at resonance. The energy range of the neutron resonances of most common elements spreads in the few MeV range, with different bins corresponding to neutron time of flight (TOF) values. Taking radiographs at specific TOF windows for the neutron absorption resonances, the sample geometry and composition could be revealed. It is thus important to have a small uncertainty of the neutron emission time, the main parameter impacting the resolution of the method. In consequence, the short time scale of the emitted neutron bunch represents a crucial feature of the laser related technology with respect to other types of neutron sources based on conventional accelerators, capable to provide neutron pulse duration in the nanosecond scale. Preliminary, we estimate few times 10^{10} neutrons per shot emitted isotropically at ELI-NP, produced via photonuclear reactions.

The nuclear physics experiments described above will take place in E1 experimental area. In the first phase of implementation the interaction chamber will host in various configurations up to one flat mirror and one F/3 off axis parabolic mirror for each of the two high power laser beams.

The dimensions of the vacuum chamber are $L \times W \times H = 3\,m \times 3.5\,m \times 1.8\,m$. Most of the experiments require a solid primary target for particle acceleration and a secondary target where nuclear reactions occur. Thin films are the basic choice for proton and heavy ion acceleration, but also metallic foams and 3D structured target will be employed attempting to optimize the yield or divergence of produces particles. A well-equipped target laboratory within ELI-NP facility will assure the fabrication, characterization and micro-assembling of multi-targets. The secondary target might be gaseous or solid (thick) foil to be replaced at different frequency compared to primary target which is destroyed at each laser pulse. A versatile remote controlled target exchange system is foreseen to be installed on top of interaction chamber above primary and secondary targets. It will not only diminish the number of venting-pumping cycles of the large interaction chamber, but will contribute also to reduction of total dose uptake reducing human interventions in vicinity of activated materials around the target.

Beside laser diagnostics and target alignment systems, the experimental equipment include plasma diagnostics, XUV imagistic instruments and spectrometers, passive and active detectors for particles and gamma radiation. However, some of the special devices mentioned through this section will be developed and installed only depending on the success of optimization of acceleration schemes. The proposed x-ray backlighter is expected to contribute to understanding laser solid target acceleration mechanism providing insight on high density plasma evolution and parameters. Based on betratron radiation emitted in laser wakefield electron acceleration process in low density (sub-critical) gas targets, the x-ray backlighter will be produced though a small pick-up from the main beam driven into a gas cell generating coherent radiation in the range of 5-20 keV range approximately [37] thus enabling x-ray radiography and deflectometry with fs time resolution and μm space resolution of plasma created by the main beam—target interaction.

2.3. Electron acceleration and gamma production in a laser-plasma interaction

The two 10 PW laser beams are steered by the laser beam transport system also to the E6 experimental area, devoted to investigation of new, fundamental phenomena of quantum electrodynamics (QED) in the strong electromagnetic fields created by high power lasers [38].

A source of high brilliance, mono-energetic gamma beams can be developed based on photon Compton inverse scattering off a relativistic electron beam, similar to ELI-NP GBS machine (see section 3), but using laser accelerated electrons. High quality, monoenergetic electron beams with energies up to several GeV has been obtained [39, 40] at existing 1 PW facilities using laser wakefield acceleration (LWFA) mechanism in (low density) gas targets and energies of few tens GeV (corresponding to Lorentz factor $\gamma > 10^4$) are expected at ELI-NP. The main experimental challenge proved to be the pointing stability of the two beams (electron and scattered laser) and their temporal synchronization.

As intensity of the laser interaction with electron beam increases, the non-linear Compton scattering regime and then radiation reaction are more and more important, the resulting gamma energy distribution changing from a photon energy upshift with the $4\gamma^2$ factor to a very broad, synchrotron like spectrum. As an example, in [41] are estimated 10^{11} photons in a synchrotron like spectrum peaking at 10 MeV with about 2% conversion efficiency of laser energy to photons, for typical LWFA electron beam of 200 MeV colliding a 5×10^{21} W/cm^2 laser pulse.

Hard X-ray up to a few MeV gamma are produced in LWFA also through resonant betatron emission of the electron bunch due to its wiggling in the plasma wake during the acceleration, using, therefore a single laser pulse and a gas target. However, the flux of high energy gamma is orders of magnitude lower [42].

Much higher gamma fluxes are expected at focalization of ELI-NP 10 PW pulses on solid targets at intensities around 10^{23} W/cm^2. Gamma emission conversion efficiency is predicted to reach up to 30% of laser energy [43] due to new mechanism associated to relativistic transparency induced in overdense targets and extremely high laser and plasma fields.

2.4. Combined laser-gamma experiments

One of the features of ELI-NP that make the new infrastructure unique worldwide is the ability to use in experiments both the high power laser beams and the high intensity gamma beam (or the electron beam from the GBS linac). These experiments, which will be performed in the E7 area, aim to tackle outstanding problems in fundamental physics and nuclear astrophysics.

This type of experiment proposed in the ELI-NP Technical Design Report [44] are phased, following increasing complexity, for both E7 and E4 areas. In E7 the experiments proposed for the beginning of operation are the production and photoexcitation of isomers (PPEx). These will be followed by experiments for the study of pair production and vacuum birefringence effects.

The PPEx requires the loose synchronization between the laser and gamma beams, the latter being used as a probe beam at milliseconds after the laser shot. The experiments for producing the isomers may be performed either by multiple laser shots (lower power but higher repetitions rate, such as 1 PW/1 Hz) or a single laser shot of the 10 PW lasers. An isomer is produced in the inelastic electron scattering or in a photoabsorption reaction, leaving the nucleus in either bound or unbound states; the bound states decay to the isomeric state via γ-transition, while the unbound states undergo neutron emission followed by γ-transition to the isomeric state. Laser-accelerated electrons to energies less than a few tens MeV will produce Bremsstrahlung radiation that would most effectively produce isomers in the final target. Therefore, a key technology is to produce a vast number of MeV electrons by laser acceleration suited to the production of isomers, and for that purpose various methods of acceleration in gas and solid targets are under investigation at the present time. Photoexcitation of isomers is verified by detecting

photoneutrons. For example, the $^{155}Gd^{m}$ isomers with the spin-parity of $11/2^{-}$ and the excitation energy of 121 keV are photo-excited just above the neutron threshold at 6635 keV by a highly monochromatic gamma-ray beam with an energy spread <0.5% (33 keV) in FWHM at energies between 6514 and 6635 keV. Thus, photoneutron emission occurs on ^{155}Gd not in the ground state but in the isomeric state. The neutron detection is carried out in collaboration with the instruments proposed in the section 3.7.3.

2.5. Irradiated materials science

The E5 experimental area will host an experimental set-up for two 1 PW peak power synchronous pulses running at 1 Hz. The area was designed to work in the parasitic beamtime mode, following a particle accelerators model. One of the laser beams will be used with f/20 focusing optics for interaction with gaseous targets while a shorter focal distance parabola will mainly use liquid or solid density targets. In this way one can expect to easily produce electrons with energies of about 500 MeV. Above to 2 GeV the electron bunches are obtained with long focal distance parabola, together with secondary radiation such as betatron radiation or bremsstrahlung radiation. With the short focal distance parabola, protons and light ions can also be produced, with energies in the range of 20 MeV and, subsequently, neutrons could be generated using various converters such as Beryllium targets.

A number of subjects related to the above mentioned radiation sources were identified for the early experiments at E5, including studies of materials behavior in extreme environments for particle accelerators such as super-FRS target at FAIR [21] or secondary collimators for HL-LHC [45]. This domain of R&D includes tests and development of detectors suitable for short radiation bursts with durations below microsecond where detection is difficult and when standard electronic driven detectors are not appropriate due to high radiation flux. Evaluation of high energy ionizing radiation effects in materials, testing of irradiated optical components, studies of materials for nuclear facilities and finally studies concerning biological systems under irradiation will be the main R&D subjects under investigation at E5.

3. Nuclear physics with brilliant and quasi monochromatic gamma beams at ELI-NP

3.1. The gamma beam system (GBS) of ELI-NP

ELI-NP will host a highly versatile gamma beam system (GBS) providing gamma rays with continuously tunable energy in the range from 200 keV to 19.5 MeV. Production of gamma beams is based on the Inverse Compton Scattering (ICS) of laser light pulses on relativistic electron bunches. The ICS process is the most efficient process to produce gamma rays following the Doppler up-shift of the laser frequency. The shortcoming of the method stays in the reduced cross section of the process (of the order of 10^{-25} cm^2) and for the practical reasons of producing high-intensity gamma beams one needs to maximize the number of colliding photons and electrons in a small spatial volume. In the case of ELI-NP this will be achieved by using high quality interaction lasers delivering high brilliance high repetition light pulses and a low-emittance high-intensity warm radio-frequency (RF) linear electron accelerator. The design and construction of the ELI-NP GBS was assigned to a European Consortium of academic and research institutions and industrial partners, called EuroGammaS [46]. The system will consist of two stages: a low-energy stage delivering gamma rays with energies up to 3.5 MeV and a high-energy stage where the energy of the gamma rays will reach up to 19.5 MeV. A schematic layout of the GBS in the ELI-NP building is shown in figure 4; the two stages and the main components of the system are marked on the figure.

In designing the system several new concepts were developed to ensure the delivery of the gamma beams with parameters that will make this system the new state-of-the-art facility for gamma beams in the world. The spectral density and bandwidth of the gamma beams to be provided at ELI-NP are compared with other facilities around the world in figure 5.

The main components of the GBS are as follows:

- *The RF linear electron accelerator.* Electrons are generated by a high luminosity RF photo-injector composed of a new concept multi-bunch photo-gun [47] and two S-band accelerating structures similar to the SPARC project at INFN Frascati [48]; the photo-cathode laser will deliver trains of 32 pulses in the UV domain and with picosecond duration at a repetition rate of 100 Hz; electrons will be generated in trains of 32 bunches of 250 pC charge each, separated at 16 ns, and repeating every 10 ms; acceleration of the electrons will be performed with specially designed C-band accelerating structures [49]; the electron beam will be characterized by outstanding features such as: normalized emittance of about 0.2-0.6 mm·mrad, bunch energy spread of 0.04-0.1%, time arrival jitter of less than 0.5 ps and pointing jitter of 1 micron; the accelerator is designed in two stages, a low-energy one delivering electrons with energies up to 300 MeV and a second one where electrons will reach energies higher than 720 MeV;
- *Interaction lasers.* The interaction lasers are of cryo-cooled Yb:YAG type, operating at 100 Hz and delivering green light pulses (515 nm) with 200 mJ energy. There are two such interaction lasers. One is used for the low-energy interaction point. At the high-energy interaction point, to ensure the high spectral density of the gamma beam, both lasers will be used.
- *Laser beam circulators.* Since electrons are produced every 10 ms in trains of 32 micropulses separated at 16 ns one from the other and the interaction lasers will provide pulses every 10 ms there is the need to circulate the laser pulses 32 times such to bring them to the interaction point for every electron micropulse; the very low cross section of the ICS process ensures that the number of photons in the laser pulses after every interaction will be practically

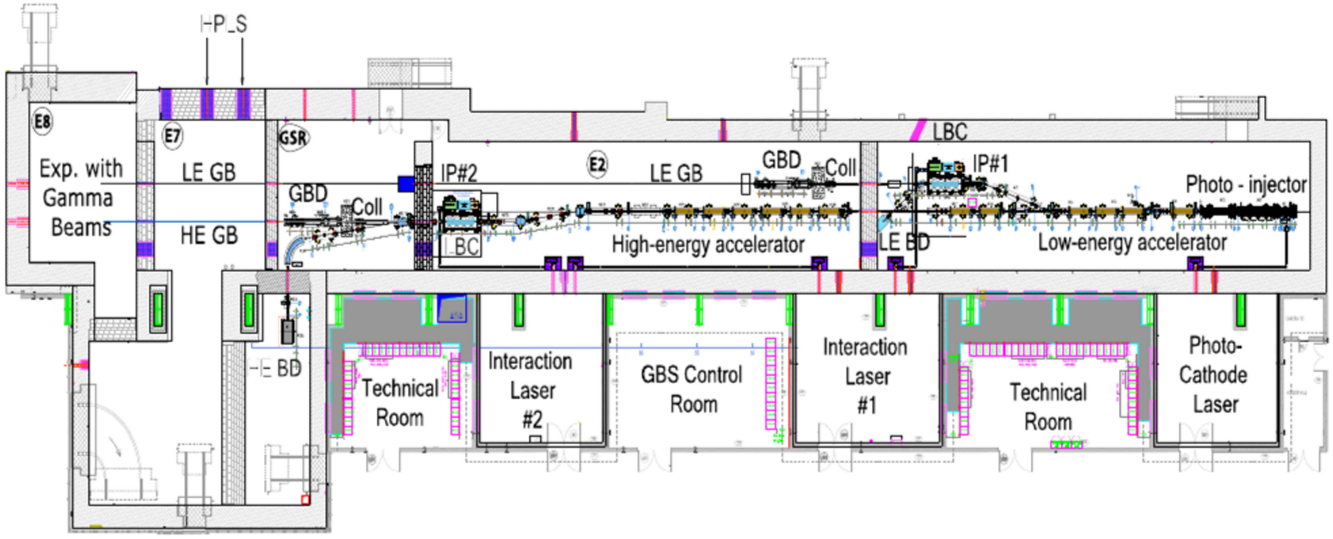

Figure 4. General layout of the ELI-NP Gamma Beam System. The components of the system are marked on the figure (LE = low energy, HE = high energy, GB = gamma beam, GBD = gamma beam diagnostics, Coll = collimator, IP = interaction point, LBD = laser beam circulator, BD = beam dump). The experimental rooms where gamma beams will be used are also marked on the figure (E2, GSR, E7, E8).

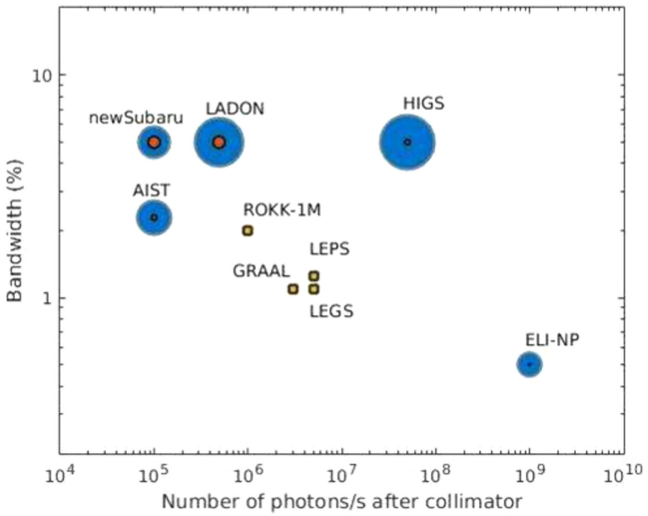

Figure 5. Comparison of ELI-NP with several other gamma beam systems around the world (LADON [50, 51], LEGS [52], HIGS [53], GRAAL [54], ROKK [55, 56], LEPS [57, 58], NewSUBARU [59], AIST [60]. The two main parameters, bandwidth and number of photons after the collimator (on target) are presented. The size of the external disks represents the maximum attainable energy, while the inner disk represents the minimum operating energies. Represented with yellow squares are the systems with an energy range outside the 1-100 MeV.

unaltered; circulation of the laser beams will be performed in high quality optical resonant cavities without sensitive degradation of the pulses intensity and duration and preserving the polarization of the photons [61];

- *Gamma beam collimators.* The scattered photons after the ICS process cover the full energy range from almost zero to a maximum value of about $4 \cdot \gamma^2 \cdot E_L$ where γ is the Lorentz factor and E_L is the laser photon energy; to select photons within a narrow energy bandwidth one has to make use of the energy dependence of the gamma-ray photons on the emission angle; by placing a collimator in front of the gamma beam one can select a small angular opening of about 100 msr around the beam axis to obtain a relative bandwidth lower than 0.5% while the spectral density of the beam will be of about 10^4 photons/s·eV; a versatile collimation systems was designed for the project [62] with continuously adjustable aperture to provide the same parameters of the beam for all the gamma beam energies;
- *Gamma beam diagnostics.* Optimization of the gamma beam production is done with a dedicated diagnostics setup composed of several detection setups; the energy of the beam will be monitored with a combined system of detectors using nuclear resonance fluorescence (NRF) and Compton scattering on thin targets; the intensity of the beam will be measured with a calorimeter composed of stacks of plastic converters and Si detectors; the gamma beam profile will be recorded with a CCD camera after a scintillator thin panel [46].

The main features of the gamma beams to be provided at ELI-NP are summarized in table 1. Such outstanding features will contribute to the revival of nuclear physics experiments with electromagnetic probes by opening new possibilities in nuclear photonics and astrophysics studies and in a wide range of applications.

3.2. NRF experiments with gamma beams

The NRF method consists of the excitation of nuclear states below the particle separation threshold through resonant photo-absorption of gamma rays and the subsequent re-emission of gamma rays following the decay of the excited states. The advantage of using electromagnetic probes to study nuclear structure is that the interaction is well-known and one can determine in a model independent way the observables relevant for understanding the nuclear structure.

Table 1. The parameters of the gamma beams at ELI-NP Gamma Beam System (GBS).

Gamma beam parameters	Value
Energy [MeV]	0.2-19.5
Spectral density [photons/s/eV]	$>0.5 \cdot 10^3$
Bandwidth [%]	$\leqslant 0.5$
Peak brilliance [photons/s·mm^2·mrad^2·0.1% bdw]	10^{20}–10^{23}
Pulse length rms [ps]	0.7-1.5
Linear polarization [%]	>95
Macro repetition rate [Hz]	100
Number of pulses/macropulse	32
Pulse-to-pulse separation [ns]	16

The NRF method provides information on excitation energies, gamma-ray transition energies, spins and parities of excited states. Accurate measurements of the photon scattering cross-sections allow for a model independent determination of radiative widths, and hence reduced transition probabilities and lifetimes.

The first results from pioneering work using the NRF method were reported as early as 1951 [63]. Since then the development of gamma-ray sources has gradually transformed NRF in a useful and reliable tool for nuclear structure studies. The advent of facilities producing high-intensity broad-energy bremsstrahlung radiation allowed in the 80's the discovery and study of a new type of nuclear excitation, the scissors mode [64]. Multi-phonon states such as the $2^+ \otimes 3^-$ quadrupole-octupole coupling [65, 66] can also be identified and characterized with the NRF method.

The development in the 90's of gamma beam systems based on laser Compton backscattering (LCB) providing quasi-monochromatic beams with tunable energy, high degree of polarization and sufficiently high spectral density has marked a qualitative jump in the experimental studies of nuclear structure with NRF. These beams will selectively populate the excited states of interest while a strong reduction of the background from the scattering of the non-resonant photons will be achieved. The high degree of polarization of the gamma beams will allow for high sensitivity parity measurements. The first experiments with completely polarized LCB gamma beams were performed at the National Institute of Advanced Industrial Science and Technology (AIST) [67].

The present-day state-of-the-art gamma beam system is high intensity gamma-ray source (HIγS) at the Triangle Universities Nuclear Laboratory (Duke University) [53]. Nuclear structure investigation with NRF is an important component of the scientific program at HIγS and resulted in numerous published results [68–75].

The superior features of the gamma-ray beams such as tunability over a wide range of energies, narrow bandwidth, high spectral density, and high degree of linear polarization, make of ELI-NP a unique facility to investigate challenging problems in nuclear physics and NRF is one of the main tools proposed to be used (see [76] for a detailed description).

The outstanding features of the ELI-NP gamma beams make them an ideal probe for non-destructive and non-invasive investigations in a broad range of fields. The various applications intended to be developed at ELI-NP target to use NRF and computed tomography (CT) to provide unique opportunities for industry and society [77].

3.2.1. Nuclear structure studies at ELI-NP interest. NRF experiments will be performed in two experimental areas of the ELI-NP main experimental building: the E2 area where low-energy (up to 3.5 MeV) gamma beams will be available and the E8 area where both low- and high-energy (up to 19.5 MeV) gamma beams will be delivered. Gamma beams at ELI-NP will allow for the study with an unprecedented resolution of the pygmy dipole resonances (PDR) in nuclei. The new information will be used to test the Axel-Brink hypothesis that resonance structures should be built on excited states the same way as on the ground state [78, 79]. Moreover, the new experimental data will be valuable contribution to the discussions on the role of E1 response of nuclei in constraining the symmetry energy parameters in the nuclear equation of state [80, 81].

The self-absorption method [82, 83] allows for a model independent determination of the absolute ground-state transition widths Γ_0 and total transition widths Γ. NRF measurements are sensitive to the product between the ground state width Γ_0 and the branching ratio Γ_0/Γ. It was recently shown [84] in an NRF experiment performed at the bremsstrahlung facility of S-DALINAC that by combining the use of monochromatic gamma beams with high-resolution gamma-ray spectroscopy one can determine the Γ_0 for individual states even in the case of high level density regions such as the PDR region.

The NRF method will provide important information about the nuclear structure of the irradiated nuclei allowing for the study of their dipole response. High resolution systematic scans in excitation energy of great interest for studying the E1 excitation strength around the pygmy (PDR) and giant (GDR) dipole resonances energy region will be performed. The results will be used to further constrain the parameters used in state-of-the-art theoretical calculations. An important question in this respect is the amount of branching transitions from dipole excited states in the PDR region to lower-lying excited states. Such low energy γ-decay branches are difficult to observe but they directly re-scale the observed E1 excitation strength. Due to the high brilliance of the beam, selection of either individual excited states, or very narrow averaging bins can be achieved, revealing information on the fine structure of the E1 strength distribution at PDR energies.

Population and decay pattern of 2^+ nuclear excited states members of rotational band structures built on scissors mode states will provide new information of the E2 strength of the scissors mode. Quadrupole-octupole phonons coupling in nuclei results in a multiplet of states with spins and parities $J^\pi = 1^-, 2^-, 3^-, 4^-, 5^-$; the NRF method would allow for a systematic identification and study of the decay of the 1^- states members of the multiplet.

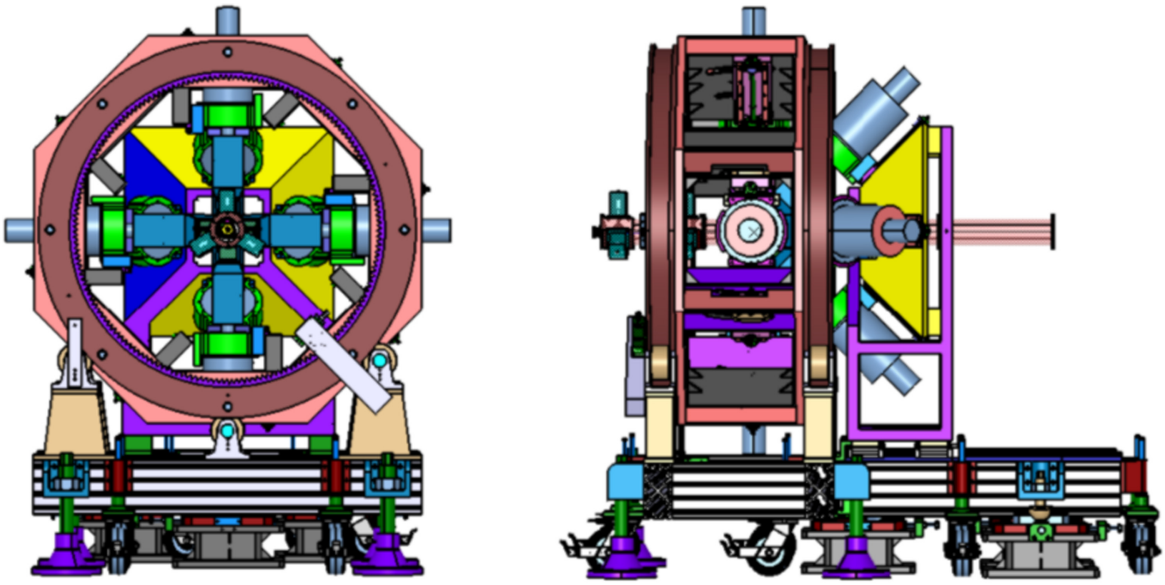

Figure 6. CAD design of the ELIADE Clover Ge detector array at ELI-NP.

Features of the gamma beams available at ELI-NP such as high brilliance and small transversal diameter will provide an increase in sensitivity of the measurements leading to a drastic reduction of the material quantities required for the construction of the targets. This opens the possibility to study rare nuclei available in nature in very limited quantities such as the p-nuclei; there are 35 known p-nuclei and at ELI-NP it will become possible to study their dipole response. Actinide nuclei due to their natural activity are difficult to use in large quantities because of radioprotection regulations and the generation of large radiation background that blinds the γ-ray detectors; their study will become possible at ELI-NP where only very low quantities of target material will be needed. This will permit a systematic study of their dipole response including octupole-quadrupole phonons coupling and low-lying scissors like resonance [85].

The main experimental setup proposed for NRF experiments is an array composed of eight HPGe segmented CLOVER detectors similar to the ones used in the TIGRESS setup at TRIUMF [86]. The array is called ELIADE (**ELI**-NP **A**rray of **DE**tectors) [76]. Every single HPGe crystal of the CLOVER detectors has eight segments resulting from a combination of one transversal segmentation and a four-fold longitudinal segmentation.

In defining the geometry of the CLOVER detectors in the array one has to keep in mind several particular requirements related to the use of high-intensity polarized gamma beams. First of all, the scattering of gamma rays in a forward direction will blind the detectors and consequently no detectors were located below 90o azimuthal angle. In order to take advantage of the linear polarization of the gamma beam to determine the character, electric or magnetic, of the emitted gamma rays one has to place detectors in the polarization plane and perpendicularto it [86]. Moreover, to determine also the multipolarity of the gamma-ray transitions one needs to perform an angular distribution analysis of the gamma rays. The CAD design resulting from detection geometry optimization based on Monte Carlo simulations with the GEANT4 code [76] is shown in figure 6. The mechanical support structure is designed to host up to twelve CLOVER detectors but for the Day-1 experiments a configuration with four detectors at 90o and four detectors at 135o will be implemented.

3.2.2. Industrial applications. While NRF applicability has been probed in fields related to safeguard and nuclear waste management, in other fields like cultural heritage, medical diagnostics, and food industry is yet to be demonstrated. The high-intensity, energy-tunable and monochromatic features of an ELI-NP gamma beam coupled with the high-efficiency of the ELIADE gamma array detector will meet the criteria for high sensitivity NRF measurements that are crucial in some of the above-mentioned fields. Moreover, the NRF method used in combination with radiography and tomography can produce isotope-specific mapping or 3D elemental/isotope imaging in various objects [77, 87]. Accordingly, the radiography and tomography setups to be developed at ELI-NP are designed to perform high-resolution scans of objects up to 150 kg and one meter wide.

An estimate on the performance of the experimental setups dedicated to an industrial application of gamma beam at ELI-NP was carried out by using analytical methods and numerical simulations [77]. For the NRF-based investigations we considered both scattering and transmission NRF experiments, and the estimations were compared with a recent experiment at HIGS [88]. The case study used for comparison is the detection of special nuclear materials (SNM) that are hidden in high-density matrices. Using the same surrogate materials as in [88] and a high-efficiency gamma array like ELIADE, same statistics as at HIGS can be achieved at ELI-NP in less than two minutes [77]. The three orders of magnitude difference can be roughly attributed to the

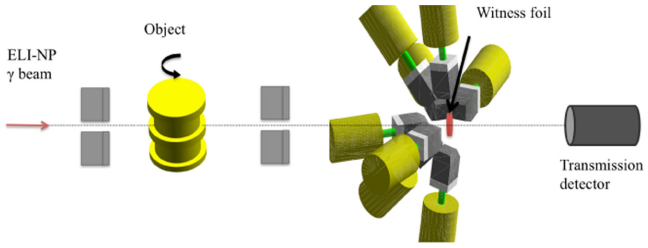

Figure 7. Schematic view of the transmission NRF setup proposed for applied physics studies to be performed at ELI-NP with gamma beams.

difference in the magnitude of the gamma beam intensity and the higher efficiency of the detector array. For the tomography and radiography setup we estimate the spatial resolution and the contrast sensitivity using line-pair structures (line pairs per mm—LPM). The collimated beam intensity is a few order of magnitude higher than any other gamma-ray source available worldwide increasing substantially the size of the investigated objects and the imaging resolution [77]. To examine the feasibility of CT imaging of specific isotopes in highly dense objects at ELI-NP, a simulation study was performed [89] using the design values of the gamma beam [87].

One of the proposed experimental configurations at ELI-NP using the NRF transmission method is shown in figure 7. Here, the ELIADE array is placed downstream of the investigated object and measures the attenuation of the resonant photons in the witness foil. The preferential attenuation of resonant photons in the witness foil is correlated with the presence of a particular isotope in the object. A detector placed in beam, downstream of the witness foil, measures the transmitted radiation. For radiography and computed tomography, two automated positioning systems capable of biaxial translation and rotation will be available for placing objects with high accuracy in beam.

3.3. New perspectives in photofission research

Brilliant quasi-monochromatic gamma beams, produced in laser Compton backscattering (LCB), provide a new perspective for photofission research, as high-resolution studies become possible. The photofission experimental program, which is in preparation at ELI-NP [90–92], will address investigations of the fission potential-barrier landscape in the actinide nuclei. The experiments will address studies of angular, mass and charge distributions of fission fragments and measurements of absolute photofission cross sections. Rare photofission events, such as high-asymmetric fission or ternary fission will be investigated, too.

The production of brilliant narrow-bandwidth gamma beams enables a major step forward in quest for extremely deformed nuclear shapes in the light actinides through studies of transmission resonances in the prompt fission cross section [93, 94]. In these experiments, the landscape of fission potential energy surface (PES) can be studied by measuring the fission probability as a function of the excitation energy. When the energy of the nuclear system is below the maximum of the fission potential barrier, the nuclear wave

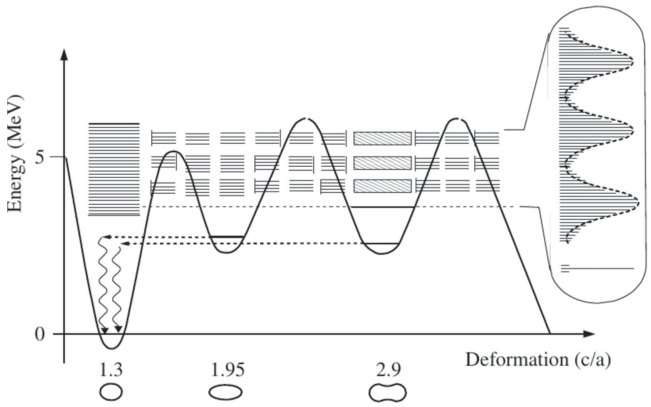

Figure 8. Schematic description of the occurrence of transmission resonances in prompt fission through a triple-humped fission barrier. Reproduced with permission from [95]. Copyright EDP Sciences - Web of Conferences 2012.

functions is localized within one of the minima of the deformed potential, resulting in discrete states, as schematically presented in figure 8. However, they penetrate the inner barriers and there is certain mixing between excitations in the different wells of the multi-humped barrier, which is defined by the penetrability factors. Thus, in the case of a complex multi-humped fission barrier, the transition states appear as a result from coupling of states originating from different minima. They demonstrate themselves as sharp resonances in the prompt fission cross section. The occurrence of transmission resonances, caused by resonant tunnelling through excited states in the second and the third minima of the potential barrier, is presented schematically in figure 8. Their observation will make possible the identification of the excitation energies of states in the different minima of the potential barrier. Such studies will provide a better understanding of the landscape of the potential energy surface (PES) in heavy atomic nuclei.

Studies of the complex multi-humped PES in atomic nuclei have focused considerable interest during the years. In the actinide nuclei, the appearance of a deep superdeformed (SD) minimum in the potential energy surface (PES) has been observed experimentally [96] and described theoretically long time ago [97]. On the other hand, the existence of a third minimum in the fission barrier at extremely large deformation is a long-standing problem, which still awaits its solution. The situation is unclear both theoretically and experimentally. On the theory side, a shallow third minimum in the PES at large quadrupole and octupole deformations has been suggested long ago [98–100]. Recently, different theoretical approaches, e.g. microscopic-macroscopic and self-consistent calculations, did not report the existence of such minimum [101, 102]. Experimentally the situation is also not well defined. Transfer reactions [103] and photofission measurements [104–107] were explored for searches of transmission resonances. In transfer reactions, states with various spins and parities are excited. They are not very sensitive to states of any particular spin and parity, I^{π}, except for the lowest transition state which has spin-parity $I^{\pi} = 0^{+}$. Photofission

measurements are simpler to interpret since photons excite only dipole and quadrupole states with appreciable probability. In first experiments, sub-barrier photofission was studied in bremsstrahlung experiments. In these experiments, the fission cross-section is convoluted with the spectral intensity of the photon beam, resulting in a typical effective γ-ray bandwidth of $\Delta E/E \approx 6 \cdot 10^{-2}$. In ^{238}U and ^{232}Th, as well as in other even-even nuclei, plateaus a few hundred keV wide have been observed between 5.1 and 6.0 MeV. This plateau in the sub-barrier fission cross section, which is referred to as the isomeric shelf, is understood as a result of the competition between prompt and delayed fission [104, 105]. It has been suggested that $I^{\pi} = 2^{+}$, $K = 0$ resonance levels occur near 5.0 and 5.6MeV in ^{238}U and ^{232}Th, respectively, and that $I^{\pi} = 1^{-}$, $K = 0$, 1 levels occur in the region 5.5 to 6.3 MeV in both nuclei. The next experimental step was the investigation of the sub-barrier fission cross section $E \approx$ 5–6 MeV in high-resolution photofission experiments. The measurements provide evidence for the existence of narrow resonances [106, 107]. In these experiments improved energy resolution was obtained with a bremsstrahlung monochromator. The incident electron beam with energy E_i is focused on a thin converter. A fraction of the electrons ($\sim 10^{-3}$), after producing a photon of energy $E_\gamma = E_i - E_s$ in a cone in forward direction, leave the convertor with energy E_s. The detection of an electron of energy E_s, tags the photon, determining its energy and formation time. Thus, the photofission cross-section of ^{232}Th was measured with 12-14 keV resolution using tagged photons [107]. The measurements confirm three plateaus 5.20 to 5.80, 5.90 to 6.15, and above 6.30 MeV, which were reported previously [108, 109]. For each of them resonance structures was observed. In particular, well-resolved peaks, separated by ~100 keV, at 5.50 and 5.60 were observed on the lowest plateau, and at 5.92, 6.03 and 6.11 MeV on the middle plateau. Clearly, these experiments have pushed the bremsstrahlung technique to its limit, without providing a solution.

All these call for new high-resolution studies of the photofission cross section in the light actinide nuclei. In a recent experiment at the HIγS γ-beam facility, the prompt photofission cross section below 6 MeV in ^{238}U, was measured. The results indicate that the third minimum is as deep as the second one [110]. However, the bandwidth of the gamma beams at the existing facilities are not good enough for studies of the sub-barrier fission resonance structure. Such experiments can be realized taking advantage of the brilliant quasi-monochromatic gamma beam at ELI-NP, which will provide the required gamma-ray flux and bandwidth for identification of sub-barrier transmission resonances in the fission decay channel with integrated cross-sections down to $\Gamma\sigma \sim 0.1$ eVb, where Γ is the resonance width.

The experiments require gamma beams with small-size beam spot at the target position. The spatial distribution of a γ beam with a 0.5% bandwidth at a target position of the array, which will placed about 30 m away from the LCB interaction point, is presented in figure 9. The experiments at ELI-NP will benefit from the relatively small beam spot in two ways. First, smaller-size targets, using less material, will be needed,

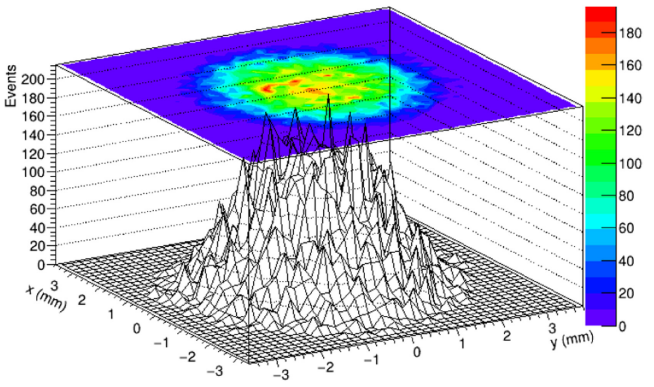

Figure 9. Space distribution of the beam spot at the target for transmission resonance experiments. Reproduced with permission from [90]. Copyright the Romanian Academy 2016.

which is an important issue since actinide targets will be used, and second, the geometry of the fission events will be determined much better, which will result in an increased precision of the experimental results.

New beyond state-of-the-art instruments have to be constructed for these studies, which will provide the needed efficiency and angular, energy, mass and charge resolution. A multi-target detector array, ELITHGEM is under development, consisting of position sensitive detector modules based on the THick Gas Electron Multiplier (THGEM) technology [111]. It will be used for measurements of fission cross sections and fission fragment angular distributions. It will be possible to map fission resonances with the array, which can be a Day-1 experiment within this research program.

For studies of the properties of fission fragments, such as angular, energy, mass and atomic number distributions, a highly-efficient four-fold array, ELI-BIC, of Frisch-gridded twin ionization chambers [112], which will be used as Bragg spectrometers or Bragg ionization chambers (BIC) [113], is designed. The performance of the BIC is been tested with one-sided ^{252}Cf source. The correlation of the mass and charge of the fission fragments is displayed in figure 10. The distribution of the light and heavy fission fragments is demonstrated in the figure. For further improvement the mass and atomic number sensitivity of the array, optimization of the tracking of the Bragg curve of the ions will be done, using digital-signal processing techniques.

Another topic, which will be covered by the ELI-NP research program, are studies of exotic fission modes, such as ternary fission, Pb radioactivity and collinear cluster tripartition. Ternary fission has been studied in neutron-induced and spontaneous fission experiments, while ternary photofission has never been observed, due to the low cross section and the availability of gamma beams with limited intensity. Compared to neutron-induced or spontaneous fission, photofission studies at ELI-NP will be done with highly polarized beams, which fixes the geometry of the process. Ternary particles are released close to the scission point. Thus, they provide information about the neck, which is formed between the two fission fragments, and about fission dynamics. Therefore, it is very interesting to measure light-particle emission in

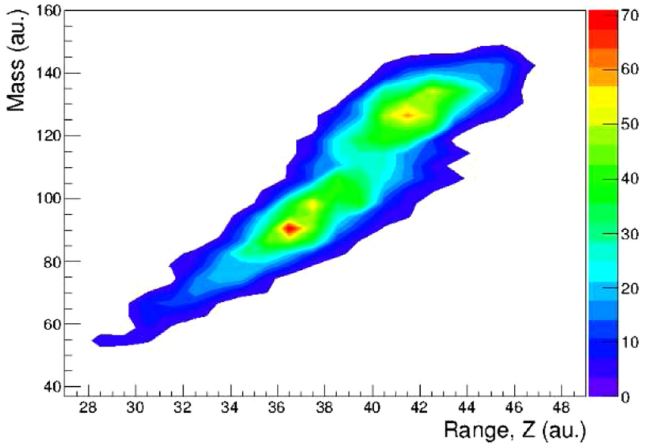

Figure 10. Experimental correlation of mass and charge of fission fragments in spontaneous fission of ^{252}Cf. Reproduced with permission from [90]. Copyright the Romanian Academy 2016.

coincidence with fission fragments. For this purpose each BIC of the ELI-BIC array will be coupled to eight ΔE-E detectors, consisting of an ionization chamber for registration of the ΔE signal and a Si strip detector for the E signal. The array will be used for identification of the ternary fission particles and for studies of their correlation with the properties of the fission fragments, such as angular, energy, mass and charge distribution. The ELITHGEM array will be used in cross-section measurements of ternary particle emission. The experiments will be carried out as a function of the energy of the gamma beam.

Other open problems, which will be addressed at ELI-NP, are the mechanism of emission of ternary particles and the role of deformation energy, the role of the spectroscopic factor, the formation of heavier clusters in ternary fission, to list a few. Measurements of light particle in photofission will shed light to problems as light-particle decay of excited states and search of enhanced α decay of extremely deformed states in the light actinides.

3.4. Production of exotic nuclear beams in photofission

Studies of neutron-rich nuclei, lying away from the valley of β stability, are the main topic of recent nuclear structure research. Beams of such nuclei are produced with the isotope-separation on-line (ISOL) technique [114], or with the in-flight separation technique in projectile fragmentation at intermediate or relativistic energies [115]. In both cases, the nuclei of interest are transported away from their production cite, where a large background from nuclear reactions exists, to a well-shielded experimental set-ups, where different nuclear observables can be measured. The transport is used also for purification of the beam and to preparation of its needed parameters with respect to energy, time and ion-optical properties for the experiments. The low yield of the isotopes of interest is a major shortcoming of the in-flight method, while not all elements can be extracted from an ISOL target due to the long diffusion times of many of them.

Photofission provides another possibility to create exotic nuclei in the laboratory. So far, photofission has been explored as a mechanism for the production of neutron-rich nuclei at bremsstrahlung facilities, such as ALTO [116] and ARIEL [117]. At such facilities mA electron beams of energies $\geqslant$50 MeV are sent on a converter, producing bremsstrahlung photons, with energies which cover the energy range of the GDR of the fissile target. Thick ^{238}U targets and the ISOL technique [114] are used.

The isotopes of refractory elements cannot be extracted with this technique. Therefore, other methods need to be used for their extraction and manipulation. Usually, the IGISOL method is used for extraction of refractory isotopes, which is based on the gas-catcher concept [118]. Within this method, the reaction products are thermalized in noble gas, He or Ar, and together with the gas part of them are extracted through an exit hole of the gas cell and delivered for further manipulation, e.g. isotope separator or a radio-frequency (RFQ) ion guide [119]. Two different techniques are used. With the first one, the ions are in 1^+ or 2^+ charge state, when they are extracted from the gas cell. In the second case, the ions are neutralized in the gas cell and these of the isotope of interest are then selectively ionized.

A problem, which needs careful consideration when using this technique, is the slowing down in the gas and the neutralization or charge reduction of the reaction products. A critical parameter in the process is the extraction time. While classical IGISOL systems [118] use noble gas circulation for ion extraction, other gas-catcher systems use electric RF and DC fields to guide the ions to the gas-cell exit hole and decrease the extraction time [120–123]. The electric fields are used also for reduction of the diffusion losses. Another problem, which might become a major bottleneck of this technique is the formation of space charge in the gas catcher, which results from the slowing-down of the ions in the gas of the cell, or can even block the extraction.

The possibility to use the IGISOL technique at ELI-NP has been explored [124]. In this case a stack thin targets are used and the ions, produced in fission, recoil out of the targets. They are slowed down in the gas and the isotopes of interest are further selected through mass separation.

At ELI-NP a γ beam, covering the energy range of the GDR will be produced through LCB. The low-energy part of the spectrum can be cut through collimation, due to the space distribution of the LCB γ-rays. The spectrum of the LCB γ beam is presented in figure 11 together with the photofission cross section of ^{238}U. With such beam settings, only γ rays that contribute to photofission, are delivered to the target. The ELI-NP γ beam will be sent on a ^{238}U target, which will be mounted in a gas cell, placed along the high-energy γ beam line of ELI-NP.

At ELI-NP the time-averaged spectral density in gamma-beam energy range of interest, $E_{beam} = 10$–19.5 MeV, is $F = (0.8\text{–}1.1) \cdot 10^4$ photons/(s·eV). The γ rate R_γ at a given energy selection of the γ beam, $\langle E_\gamma \rangle$, is $R_\gamma(E_\gamma) = F(E_\gamma) \cdot \langle E_\gamma \rangle \cdot BW$, where $F(E_\gamma)$ is the time-averaged spectral density at the gamma-beam average energy $\langle E_\gamma \rangle$ and BW

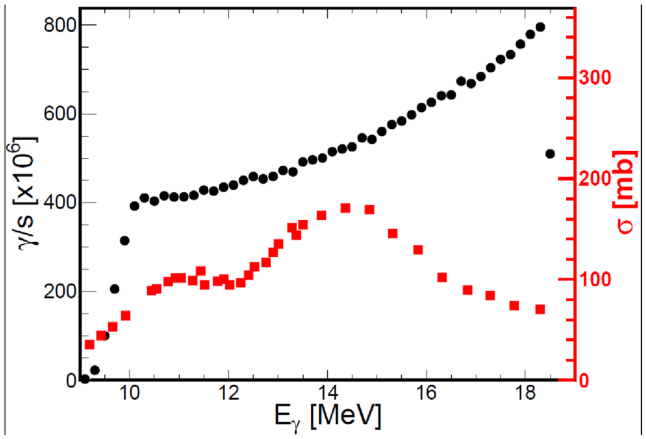

Figure 11. Spectrum of the LCB γ beam covering the photofission cross section for ^{238}U.

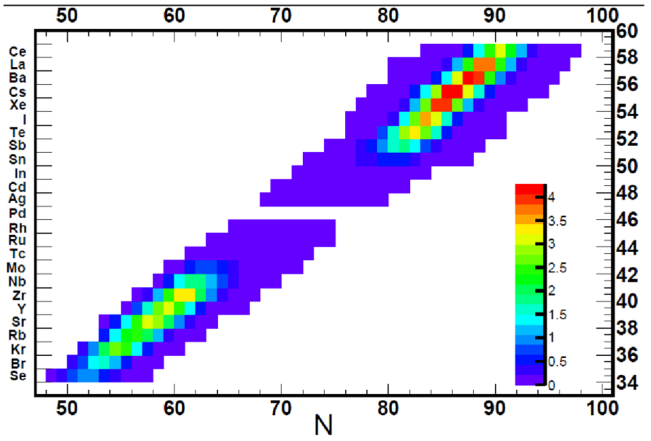

Figure 13. Estimated photofission yield distributions at ELI-NP.

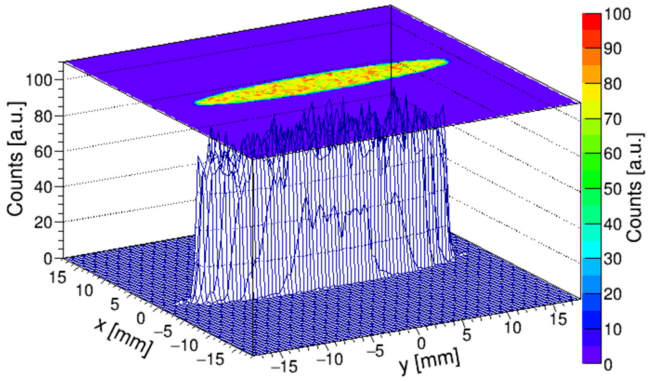

Figure 12. Beam spot at the target position for isotope-production experiments.

is the beam bandwidth. A brilliant gamma-beam of $R_\gamma(E_\gamma) = 10^{11}$ photons/s will be sent on target, choosing a setting for which the collimated gamma-beam covers the GDR of ^{238}U. In this case the collimator acts as a filter for hardening of the beam and effectively cuts the low-energy γ rays, leaving only a tiny fraction, <0.5%, resulting from scattering within the collimator.

A series of calculations aiming at a realistic estimate of the production yield at ELI-NP have been performed. Yield calculations have been performed using two independent GEANT4 applications [125]. GEANT4 is a software for the simulation of the passage (GEometry ANd Tracking) of particles through matter. Each of them is not available in the standard GEANT4 implementation, and is inheriting from the G4HadronInelasticProcess class. The cross-sections are parameterized from [126], and for E_γ= 5–7 MeV from [127]. The code, using one of the implementations, was validated in calculations of the photofission yield of the gas cell, which was proposed for the ALTO facility in France. In this case, photofission was induced by bremsstrahlung, which was produced by the interaction between the 50 MeV electron beam and a W converter [128]. A realistic beam profile at the position of the target is presented in figure 12. A gamma-beam source file, containing $4.4 \cdot 10^6$ photons, which was produced by simulating the realistic LCB interaction at the high-energy interaction point of the GBS [46], was loaded by user defined classes inheriting from the G4VUserPrimaryGeneratorAction class. In a benchmark calculation, a bulk cylinder of 800 mg ^{238}U, exposed to the high energy gamma beam with a rate of $5 \cdot 10^{10}$ γ/s, results in a fission yield of about 10^7 f/s. Thus, $6 \cdot 10^7$ f/s per gram ^{238}U are expected to occur for brilliant gamma-beam of $R_\gamma(E_\gamma) = 10^{11}$ photons/s. However, in the following calculations a more conservative value of 10^7 f/s was accepted.

The fission yields in low-energy projectile fission of ^{238}U on ^{208}Pb were measured [129], a process which takes place via exchange of a virtual photon with energy E_γ < 25MeV. The photofission yield distribution at ELI-NP, presented in figure 13, was estimated using these results. The photofission yield from [129], expressed in fragments per 100 fissions, was scaled to a total of 10^7 f/s. In the high Z region, above $Z = 56$ an extrapolation procedure, was used to extend the yield estimation. The ELI-NP IGISOL facility will focus on studies of refractory elements, which are not easily extracted at an ISOL facility. Most of isotopes of the refractory elements, lie either in the Sr-Zr or the lanthanide deformed regions, which opens an opportunity for an IGISOL experimental program at ELI-NP. These studies can address a number of key nuclear structure problems, such as e.g. the region of sudden onset of deformation in the $A \sim 100$ mass region, the structure in the vicinity of the doubly-magic ^{132}Sn and the well deformed $A \sim 150$ region.

The IGISOL beam line at ELI-NP will consist of a gas cell, where the target system will be placed, a RFQ ion cooler and analysing section, which will deliver the ions of the isotopes of interest to the measurement stations. A cryogenic stopping cell (CSC) [123, 126] is been considered. After collimation, at the CSC entrance, the γ beam will be in the energy range of 10–19.5 MeV with an intensity of about 10^{10} γ/s and a beam-spot size with FWHM $\approx$ 5 mm. The ^{238}U targets inside the CSC will have a thickness of up to 10 μm, to allow for the release of the fission fragments which are produced in the center of the target [125]. Hence, a set of thin targets will be used and, in order to avoid fragments from one target hitting neighboring targets, they must be tilted with respect to the beam, leaving some distance between two

neighbouring targets. The targets will be inclined at an angle $\theta \sim 10^{\circ}$ with respect to the γ beam, with dimensions covering the γ beam spot. The total length of the target region inside the CSC is about 1 m. More than 95% of the fragments, which are released from the targets, are stopped in about 12 cm of He gas at 70 K and 300 mbar, which implies that the diameter of the gas cell should be about 25 cm. For a gas cell with such a size described above, extraction only by gas flow would take too long for short-lived radioactive nuclei to survive. Therefore, the extraction method should combine DC and radio frequency (RF) electric fields with gas flow extraction close to the cell nozzle.

Evaluation of the target release and the gas-cell extraction were done, in order to obtain realistic estimates of the expected experimental isotopic yields, e.g. the yields at figure 13 should be corrected for the target release and gas-cell extraction. About 20% of the fission fragments will leave the target assembly [125] and about 50% of them will be extracted out of the gas cell [130] and will be transported through the RFQ ion cooler.

Isotopes, which will be produced as 10^{-3}–10^{-4} of the total fission yield, will reach the measurement stations of the IGISOL beamline at rates of 10^{3}–10^{2} ions/s, which is sufficient for *e.g.* β-decay studies. Isotopes, which are produced as 10^{-5}, will reach the measurement stations at rates of 10 ions/s, which is the limit for β-decay studies. These rate estimates are done taking into account a fission yield of 10^{7} f/s and an expected ion-survival probability throughout the IGISOL of about 10%. These intensities should be available for day-one experiments and there is room for further increase of the experimental rates with the improvement of the beam quality at ELI-NP.

3.5. Nuclear collective excitation modes

Giant resonances are collective vibrations of the nucleus, which result from the coherent contribution of many particle-hole (p-h) excitations. They can be classified depending on their multipolarity and their isovector or isoscalar nature. The giant dipole resonance (GDR) is an early discovery in nuclear physics, yet it continues to puzzle and attracts interest. The story starts with measurements of enhanced photodissociation cross section [131], which was explained by a dipole oscillation of the protons against the neutrons [132]. It continues with the observation of strong absorption of incident photons in photon-induced reaction at energies of about 15 to 20 MeV [133], which again was interpreted as excitation of a collective nuclear vibration of the protons against the neutrons [134]. The phenomenon was called GDR and it turned out to be a general feature of atomic nuclei. Most of the studies related to the GDR come from photonuclear experiments, due to the high sensitivity of photoabsorption to E1 transitions.

This dipole collective vibration of the protons against the neutrons nearly exhausts the nuclear photo-absorption cross section and is understood as isovector giant dipole resonance (IVGDR). Experimentally, the best way to investigate the nuclear collective mode is in photoabsorption experiments with polarized narrow-bandwidth γ beams, which will be delivered by the ELI-NP GBS. The information, which such experiments yield is important in several aspects. First, for understanding the effective proton-neutron interaction. This is due to the fact that when high-energy photons impinge on a nucleus, the protons feel collectively an oscillating electromagnetic field, which is essentially uniform over the nuclear volume. In the center-of-mass system, the protons are displaced with respect to the neutrons. The separation between the centers of mass of the components of the binary quantal fluid creates an electric dipole moment. On the other hand, the proton-neutron interaction acts as a restoring force. Thus, the two components of the nuclear fluid oscillate against each other. Second, the decay of the GDR to the ground and excited states in nuclei provide information of the nuclear E1 strength and the coupling of the GDR to low-frequency collective modes.

Another E1 collective mode, the pigmy dipole resonance (PDR), was suggested at the turn of the century in the energy region 6-12 MeV as collective excitation mode of a dipole oscillation of neutron-skin against a core nucleus [135]. It lies in the low-energy tail of the GDR. Understanding the PDR is important to clarify the entire E1 response of nuclei. Besides, the PDR may be a good probe of the nuclear symmetry energy in the equation of state (EOS) for nuclear matter [136].

The decay measurements are a unique way to understand the nature of the Pygmy resonance. At present, several experiments show the existence of such extra strength below the GDR region [136–138] but they are not capable to pin down its microscopic structure. Theoretically, while some models predict only single-particle, *i.e.* non-collective, excitations in that region, other models show the emergence of collective states that have, however, rather complicated structure (mixed isoscalar/isovector nature, possibly compressional and/or toroidal character). It may be expected that the decay measurements shed light on such questions.

Magnetic dipole resonance (MDR) of spin-flip type coexists with PDR around neutron threshold in the tail of GDR. MDR together with PDR constitute extra strengths of the low-energy gamma-ray strength function, which is a nuclear statistical quantity common to (γ, n), (γ, γ') and (n, γ) reactions. Recently, the gamma-strength function method has been devised to indirectly determine radiative neutron capture cross sections for radioactive nuclei relevant to the s-process nucleosynthesis and nuclear transmutation [140]. In this regard, it is important to provide MDR strength data above neutron threshold which is poorly known and is scarcer than PDR data. The highly polarized small-size brilliant gamma beam at ELI-NP will allow to distinguish between these two modes.

Exclusive measurements of the decay of giant resonances providing the values of the electromagnetic and particle decay widths are presently very few and much demanded. ELI-NP will provide intense enough γ beams for such studies. One of the main issues is whether the most appropriate effective interaction to be used in the isovector channel, e.g. in models like the random phase approximation (RPA), is established on a solid basis. For instance, in non-relativistic calculations based on the Skyrme effective interactions, the dipole

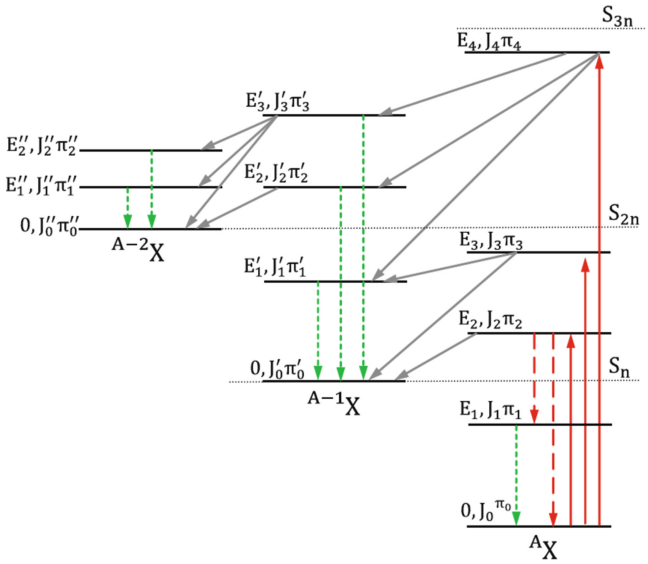

Figure 14. Schematic view of complex neutron decays of giant resonances. Reproduced with permission from [146]. Copyright Springer 2015.

spectrum is fragmented in several states. These states acquire a width in case coupling with more complex 2 particle-2 hole (2p-2h) configurations is taken into account. Fine structure is already observed in excitation experiments [141–145]. However, its counterpart, the fine structure in decay is important to be measured. Such experiments are carried out using the Gran Raiden spectrometer in Osaka, where a beam of polarized protons of 200-400 MeV was focused on a ^{208}Pb target [142], provide the excitation cross section of the GDR. However, they do not give any information on the GDR decay to ground or high lying states through gamma or neutron emission. Experiments at ELI-NP will provide complimentary experiments to, e.g. (p,p') experiments, having a similar resolution of the γ beam, as that which is achieved with protons, but, in addition, the neutron-decay branch will be measured as a function of the excitation energy. An important feature of these experiments is that it will be possible to scan the γ-neutron branching in a large energy window, including measurements close to or at S_n, where the γ decay is expected to prevail neutron decay.

The brilliant narrow bandwidth gamma beam at ELI-NP will open new opportunities for studies of collective excitations in atomic nuclei. States above the neutron separation threshold are excited in these experiments, which, alongside NRF experiments, provide complete picture of the nuclear photo-absorption process and its decay modes. The decay of excited states above the neutron threshold, S_n, is schematically presented in figure 14.

Excited states above S_n decay through neutron emission to the ground or excited states in the residual nucleus. The decay to excited states is followed by emission of cascades of γ rays. Excitations above the two-neutron separation threshold, S_{2n}, open the (γ, 2n) decay channel. The neutron decay competes with the γ-decay to ground or excited states in the target nucleus, a process which is significantly less probable. A wealth of experimental information is obtained through measurements of the energy and angular distribution of neutron and γ decays of photon-excited resonance states, such as energies of excited states, γ-ray transitions and neutron decays, neutron-γ branching ratios, (γ, xn), (γ, γ) and (γ, γ') cross-sections, absolute transitions strengths, multipolarity of reaction neutrons, multiple mixing ratios of γ transitions, spin and parity of excited states.

In order to carry out these experiments, both high-intensity beams and high-efficiency detector systems are needed. ELI-NP will provide narrow-bandwidth brilliant γ beams. In addition, new spectrometers are under construction, such as the ELIADE array [76], consisting of Clover HPGe detectors, for NRF measurements below the neutron separation threshold, S_n, and the ELIGANT-GN array [147], consisting of large-volume $LaBr_3$(Ce) detectors, Li-glass detectors and liquid scintillators, for γ-n coincidence measurements above S_n. These instruments will allow for much more precise measurements of the nuclear photo-absorption response.

3.6. Perspectives of astrophysics at ELI-NP

Astrophysics is one of the main research topics at ELI-NP, many of its sub-topics being tackled in several research programs for the experimental areas for laser-based, gamma-based, and combined laser-gamma based experiments. Studies of nuclear structure and nuclear reactions of astrophysical interest, as well as the study of plasmas in astrophysical conditions will allow for further development of present-day knowledge in these fields.

Using the gamma beam produced by the ELI-NP system, the Charged Particles working group proposed in the Technical Design Report the construction of two instruments, a silicon strip detectors array (ELISSA) and a time projection chamber with an electronic readout (e-TPC). The physics case of this TDR comprises two mains sections, one on nuclear structure, and specifically the study of clustering in light nuclei, and one on nuclear astrophysics, aimed at performing accurate measurements of (very small) cross sections of nuclear reactions relevant for stellar burning processes.

Measuring capture reactions (astrophysical) by means of the inverse photodisintegration reactions (with the ELI-NP gamma beam), has the advantage of having different systematic uncertainties than those of characteristic charged particle induced reactions measured at low energies of astrophysical interest, thus allowing to resolve conflicting data.

Direct photodissociation reactions, of a crucial importance for the study of the p-process, will also be performed at ELI-NP with the help of a 4π neutron detection array, based on ^{3}He detectors and proposed by the workgroup Gamma above Neutron Threshold (GANT, see [148]).

3.6.1. Proposed physics cases. Nuclear astrophysics needs highly accurate measurements of small cross sections for nuclear reactions of the H and He burning processes (the astrophysical S-factor defined in [149]) in order to enhance

the reliability of stellar evolution models and simulations. Part of the proposed studies with high potential impact in this field using the charged particle detectors at ELI-NP were presented in [146], namely the $^{16}O(\gamma, \alpha)^{12}C$, $^{24}Mg(\gamma, \alpha)^{20}Ne$ and p-process reactions, and some other reactions of interest were analyzed in [44].

The $^{16}O(\gamma, \alpha)^{12}C$ *reaction* The helium burning in the stellar core of massive stars ($M > 8M_{\odot}$) leads to the formation of carbon and oxygen. The ratio between the abundances of carbon and oxygen (C/O) at the end of this stellar evolution stage has been identified three decades ago, and remains today, as one of the main open questions in nuclear astrophysics [149]. The p-wave S_{E1} and d-wave S_{E2} S-factors in the cross-section (as defined in [149]) have to be determined at the Gamow peak (300 keV) for the $^{12}C(\alpha, \gamma)^{16}O$ reaction with an accuracy better than 10%. However, even the most recent measurements reported [150–154], with center of mass energies around 1 MeV, led to the determination of the astrophysical *S*-factors with low accuracies (± 40%–80%), despite the high intensities of the alpha-particle beams employed (100–500 μA), due to the quality needed for the measured angular distributions in order to separate the E1 and E2 components.

More recently it was shown [155] that in order to understand the ^{56}Ni mass fraction produced in lower mass ($M \sim 1.4M_{\odot}$) stars evolving to Type Ia supernovae, a factor is the Carbon to Oxygen ratio. The light curves from these supernovae are used as 'standard candles' in cosmology and have played an important role in the recent discovery of the accelerated expansion of the Universe [156].

A major advantage of detecting the charged particles in the e-TPC detector of the inverse reaction $^{16}O(\gamma, \alpha)^{12}C$ with respect to previous experiments based on gamma-ray detectors (for the direct reaction) is the much reduced background.

By measuring gamma-rays there were several sources of large background such as neutrons emitted from the $^{13}C(\alpha, n)$ reaction, background gamma-rays, background from cosmic rays (direct and induced) and background due to Compton scattering. The proposed experiment only aims to measure direct capture to ground state. The contribution of cascade gamma-rays [157] from the $^{12}C(\alpha, \gamma)^{16}O$ reaction (less than 5%) will not be measured in this experiment.

The $^{22}Ne(\gamma, \alpha)^{18}O$ *reaction*. The helium burning of oxygen, $^{18}O(\alpha, \gamma)^{22}Ne$, is the path to produce ^{22}Ne, that represents an important source of neutrons for the s-process in massive stars through the $^{22}Ne(\alpha, n)^{25}Mg$ reaction. Although the helium burning of oxygen was studies previously and recently two low-laying resonances were investigated [158], the uncertainties need to be reduced. A promising new path of investigation opens with the tunable, narrow bandwidth gamma beam that will be available at ELI-NP, employing the e-TPC. Operating this instrument at 100 mbar with ^{22}Ne gas, significant statistics on the 566 and 470 keV resonances will be obtained in few weeks of beamtime.

The $^{19}F(\gamma, p)^{18}O$ *reaction* The reaction $^{18}O(p, \gamma)^{19}F$ is one of the two competing reactions for the hydrogen burning of ^{18}O, and although not dominant in this respect, it is important because of the connection it makes with the NeNa cycle, providing material for the burning of ^{19}F through the $^{19}F(p, \gamma)^{20}Ne$ reaction. Also, it could be the origin of the loss of catalytic materials from the CNO cycle, and the understanding of this process is very important at relevant temperatures (below 1 GK).Several resonances dominate the $^{18}O(p, \gamma)^{19}F$ reaction at relatively low temperatures, and down to about 0.1 GK the resonance strengths have been measured [159–161]. At lower temperature uncertainties are still very high. These resonances will be studied at ELI-NP with the e-TPC operating at 100 mbar CF_4 gas, at a gamma beam energy of 8 MeV. For the very low energy resonance at $E_{c.m.} = 90$ keV and assuming a conservative beam intensity, a count rate of about 5 events per day are expected.

3.7. Proposed instruments

3.7.1. Time-projection chamber with an electronic readout (e-TPC). The time-projection chamber (TPC) is a gaseous detector in which the gas acts at the same time as target for the nuclear reaction and detection medium. A TPC with optical readout (O-TPC) was successfully used [162] in experiments at NSCL and HIGS (USA). For ELI-NP a new concept of readout was proposed, in order to eliminate some of the limitations imposed by the use of optical readout (such as the presence in the gas mixture of a component to produce luminescence). The electronic readout employs a multi-layered PCB structure with 3-coordinate charge-collecting electrode. The charge will be read by a u-v-w readout which is mounted on a circuit board using multi-layering board technology, formed by three layers of (u-v-w) grids crossed at 60°. A strip pitch of 1.5 mm will allow for a space resolution sufficient to identify also short tracks generated by the recoil in the gas (approx. 100 mbar). This read-out mechanism allows for the reduction in the number of readout channels with respect to the classical pixels design for the same area. Also, it allows for an increased readout speed and the capability to resolve more complex events.

The readout electronics for the proposed e-TPC detector is the one developed by the Generic Electronics for the Time Projection Chambers (GET) community [163]. It allows for the use of several hundred channels in a compact setup. The active volume of the chamber, in which the reaction happens and the decay products are detected, will have a length of 35 cm and a square cross-section of 20 cm × 20 cm, centered around the beam axis with two windows for the gamma beam and another on the side for an alpha source for calibration.

For the reactions of interest proposed, the eTPC will be run at pressures of about 100 mbar, in order to allow for both the recoiling nucleus and the lighter reaction product (proton or alpha) to be stopped and tracked in the chamber's active volume. A recirculating gas systems will be built for the runs with isotopically enriched gases.

The multiplication of the drifting electrons will be achieved by a sequence of gas electron multiplier (GEM) foils produced at CERN [164, 165]. Tests for the use of these foils at low pressure were performed at CERN in 2015 and

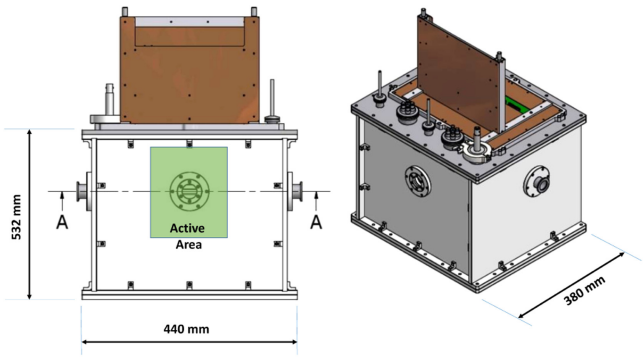

Figure 15. ELI-NP mini-eTPC detector.

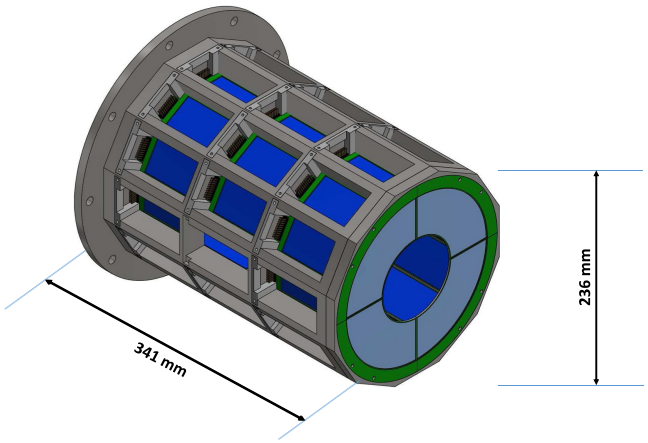

Figure 16. ELI-NP Silicon Strip Detectors Array (ELISSA).

will continue during the construction of the e-TPC. A lower scale detector, the mini-eTPC, has been built in a collaboration with University of Warsaw as a prototype for the ELI-NP e-TPC (see figure 15). It has been tested with radioactive sources and in-beam at the IFIN-HH Tandem accelerator in Magurele.

3.7.2. The silicon strip detectors array (*ELISSA*). Silicon detectors are a solution of choice for the detection of charged particles emerging in nuclear reactions because they guarantee exceptional energy resolution, have almost 100% efficiency and their thresholds can be set to very small values. Moreover, they are (almost) not sensitive to neutrons, gamma rays and electrons, which in the case of ELI-NP would constitute the beam induced background.

A silicon array makes it possible to measure reactions on solid targets, such as the ^{24}Mg(γ, α)^{20}Ne and all the reactions on heavy nuclei intervening in the p-process (^{74}Se, ^{78}Kr, ^{84}Sr, ^{92}Mo, and ^{96}Ru, for instance), thus representing a complementary detector to the e-TPC. Excitation functions and angular distributions will be measured over a wide range allowing for a better understating of the reaction mechanism. An angular coverage as large as 10°–170° can be achieved in the lab system taking into consideration the beam induced background. This coverage is large enough to perform an effective nuclear spectroscopy. Silicon strip detectors will provide enhanced angular and energy resolution with high detection efficiency. The resolution can be important for background suppression owing to, e.g., the bremsstrahlung radiation component.

The barrel can be made up of 3 rings of 12 position sensitive detectors, for a total angular coverage of 100° in the laboratory system (see figure 16). The proposed design is very compact, as the distance target—detector is about 9 cm, fixing $\Delta\phi = 6.5°$ and $\Delta\theta = 0.6°$, which is a satisfactory angular resolution for reaction such as ^{24}Mg(γ, α)^{20}Ne. Energy resolution better than 1% is measured with a calibration alpha source [166]. Since position is determined by charge partition, the number of electronic channels is strongly reduced, as about 300 channels would be necessary for the whole barrel.The angular coverage is extended down to about 20° (160° at backward angles) by using end cap detectors.

3.7.3. High-efficiency 4π neutron detector (*ELIGANT-TNH*). ELIGANT-TNH, a high-efficiency 4π triple-ring detector is proposed to tackle the Day 1 experiments regarding the ^{180}Ta(γ, n)^{179}Ta and ^{138}La(γ, n) ^{137}La reactions. *H* stands for high efficiency. ^{3}He proportional counters with the highest neutron detection efficiency per volume are the best choice in view of the rare isotope measurement and the space constraints imposed by the dimensions of the experimental hall. The ^{3}He proportional counters are embedded in a neutron moderator, with the target placed at the center of the moderator.

Each ^{3}He proportional counter is of cylindrical shape, with a 2.5 cm diameter and 49.5 cm length. The sensitive length is 45 cm. The proportional counters are placed equally spaced in three concentric rings, of 80, 140 and 200 mm diameter respectively. Ring 1 contains 4 detectors, while Rings 2 and 3 contain 8 detectors each. The neutron moderator is a cube of $36 \times 36 \times 50\,\mathrm{cm}^3$ made of polyethylene. The moderator is covered by additional 5-cmthick polyethylene plates with 1-mmthick cadmium metal for background neutron suppression. Figure 17 shows a transversal section of the neutron detector. A similar neutron detector is in use at the gamma beam line GACKO (Gamma Collaboration Hutch of Konan University) of the synchrotron radiation facility NewSUBARU [59]. Neutrons emitted in the (γ, n) reaction near neutron threshold have the average kinetic energies below 1 MeV [146, 167], and the detector has 60-74% efficiency for these. The average neutron energy is determined with the ring-ratio technique.

The moderator is designed to have a cavity on the beam axis, so that the beam can pass through the detector without intercepting moderator material. In addition to the high detection efficiency, the 3He proportional counter has an excellent capability of gamma-neutron discrimination, as the gamma pulse height is much lower than that of neutrons which is amplified by the reaction Q-value.

3.8. Production of radioisotopes of medical interest

In nuclear medicine radioisotopes are used for diagnostic and therapeutic purposes. In many medical procedures, radionuclides are combined with other chemical compounds or

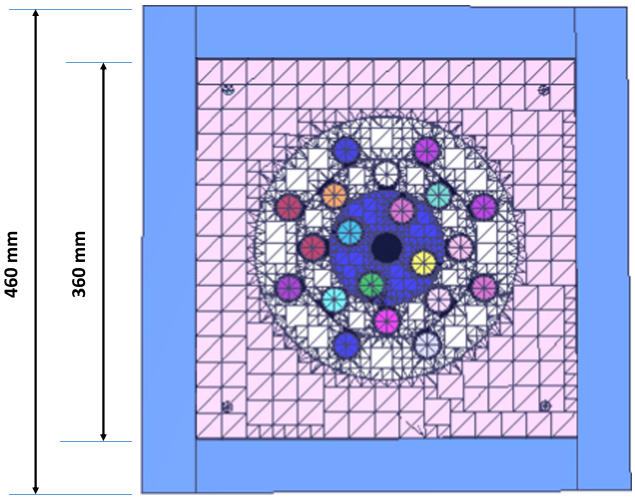

Figure 17. Transversal section of the neutron detector ELI-GANT-TNH.

pharmaceuticals to form a radiopharmaceutical which when administered to the patient can preferentially localize to specific organs or cellular receptors. This property of radiopharmaceuticals allows nuclear medicine ability to image the extent of a disease process in the body. Treatment of a disease based on metabolism, uptake or binding of a ligand, may also be accomplished. In this case, the radiopharmaceuticals rely on the tissue-destructive power of short-range ionizing radiation.

Currently, fission at nuclear reactors and proton reactions at cyclotrons are the main production technologies for medical radioisotopes [168]. The increasing demand for medical radioisotopes requires more production facilities, investigation of new production methods and the application of new radioisotopes in both diagnosis and therapy. All diagnostic methods require that the radiotracers have relatively *high specific activity*, such that the injected radiotracer is not accompanied by too many stable isotopes of the same element.

Optimization of the therapy for individual patients remains a goal of clinical practice. Development of new radiopharmaceuticals for both scintigraphy tumor imaging and systemic targeted radiotherapy and their availability are crucial factors influencing the expansion of clinical nuclear medicine [169]. Again, *high specific activities* are required for carrier-free radioisotopes used in such therapies to avoid receptors blocking with biomolecules carrying stable isotopes, thus minimizing therapeutic effects. While it may not be obvious, the choice of radionuclide is a very important decision and depends largely on the clinical utility of radiotracer. The modern approach to radiotherapy directs towards utilization of β^- particle emitting radionuclides (e.g. ^{67}Cu, ^{90}Y, ^{131}I, ^{177}Lu, ^{186}Re and ^{188}Re), isotopes, which emit Auger electron cascades (e.g. ^{111}In and ^{125}I) and α-particle emitting radionuclides (e.g. ^{211}At, ^{212}Bi, ^{213}Bi, ^{225}Ac and ^{227}Th), with high linear energy transfer in tissue, or directly in the cell. Both, methods for research studies and for clinical production of such nuclides need to be developed. The increased demand of medical radioisotopes, sets a requirement of exploring new methods for their production. One such possibility is the utilization of brilliant gamma beams [9]. Photonuclear reactions, such as (γ, γ'), (γ, n), (γ, p), with γ-beams of high intensity and large brilliance, should be explored for production of radioisotopes for medical applications, such as ^{47}Sc, ^{44}Ti, ^{67}Cu, ^{103}Pd, ^{117m}Sn, ^{169}Er, ^{195m}Pt or ^{225}Ac, with a higher specific activity than by classical methods [9, 170]. For example, ^{195m}Pt could be used to monitor the chemotherapy response of the patient to with platinum compounds before a complete treatment is performed. In targeted radionuclide therapy the short-range Auger and conversion electrons resulted from ^{195m}Pt could enable a highly localized treatment. Also, the ^{195m}Pt low-energy γ transition can be used for SPECT imaging. Recently, ^{62}Cu, ^{64}Cu, ^{124}I and ^{68}Ga are evaluated for this aim [171].

The production of *high specific activities* (A/m) is one of the most important quality criteria, which needs to be addressed when discussing a new production technique for medical radioisotopes. Here A is the produced activity and m is the mass of the target. This problem was studied recently, related to the expected brilliant gamma beams at ELI-NP [172, 173]. In these studies, a γ-beam flux of 10^{11} s^{-1} was used, which is a conservative estimate for ELI-NP. Such γ-beam fluxes will be achieved in the first phase of operation of the facility. During the operational phase of the facility, the broad-bandwidth γ beam, which is needed for these experiments, will be optimized and will result in some increase of the γ-beam flux. The interaction of the ELI-NP γ beam with solid targets was simulated, in order to estimate the production of ^{99}Mo/^{99m}Tc, ^{225}Ra/^{225}Ac and ^{186}Re.

The target geometry, the γ-beam flux, the optimization of the γ-beam energy and the convolution between the γ-beam spectrum and the reaction cross section play an important role in the determination of the maximum specific activity. Using the optimized γ-beam energy and target geometry, the saturation specific activity of the ^{99}Mo/^{99m}Tc, ^{186}Re and ^{225}Ra/^{225}Ac radioisotopes as a function of the bandwidth ratio is shown in figure 18. Here, the bandwidth ratio was defined as the ratio of the γ-beam bandwidth with respect to the reaction cross section width. The optimal bandwidth ratio was calculated to be 0.3–0.4, setting the limit at the level of a 30% drop of the produced specific activity with respect to the maximal value, which is obtained with a narrow-bandwidth beam with energy corresponding to maximal value of the cross section. This ratio may be useful for the evaluation of other radioisotope production cases.

The optimal target thickness L is correlated with the target density, ρ, for optimal production of specific activity of the radioisotope. The γ-beam is attenuated while interacting with the target and the value of the mass attenuation coefficient (μ_m) is approximately constant for a given quasi-monochromatic γ-beam and a specified target. At 70% of the maximum specific activity the target thickness satisfies the condition $L = f/\mu_m\rho$, where the factor f ranges from 0.8 to 0.9 depending on the specific radioisotope. These studies indicate that the production through photonuclear reactions

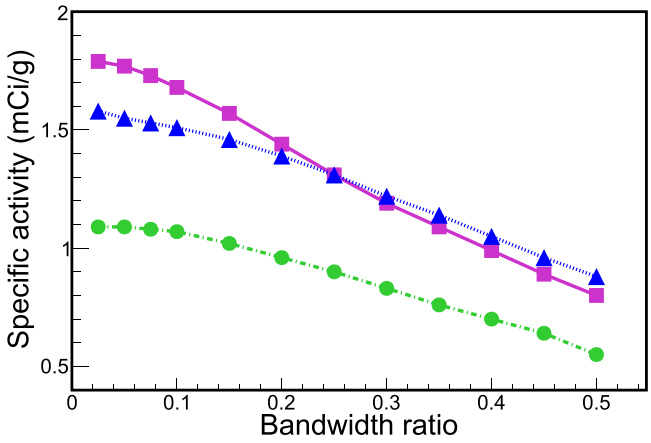

Figure 18. Specific activity of medical radioisotopes versus gamma-beam bandwidth ratio, with squares are the data for ^{99}Mo/^{99m}Tc, with triangles—for ^{187}Re and with stars—for ^{225}Ra/^{225}Ac.

possible for optimized γ-beam energy, target geometry and γ-beam bandwidth. Further, the production of isomers such as ^{195m}Pt, ^{115m}In, ^{176m}Lu and ^{87m}Sr is also of great interest. Due to a low gateway state for some key nuclides [174], it would be possible to explore the direct activation of the above-mentioned nuclides using the low-energy γ-beam, below 3.5 MeV, at ELI-NP.

Finally, various irradiation experiments of thin targets with a γ-beam, in which the specific activity of product radioisotopes will be determined, could be used to perform reaction cross section measurements. Since the ELI-NP facility could provide a much higher γ-beam flux than that produced by other available γ-beam facilities, it will be possible to make precise cross section experimental measurements for many isotopes [175], especially for those isotopes with unknown or low cross sections.

4. Conclusions

The ELI-NP facility combines two large research equipment devices with parameters beyond the state of the art, namely a high power laser system with two amplification arms to deliver 10 PW and intensities on the target in the range of 10^{23} W/cm^2 at least every minute, and a gamma beam system to deliver up to 19 MeV photons. Their outstanding performances will allow for an approach into a field of science not yet explored, at the frontier between laser, plasma and nuclear physics. This makes it possible to design and perform new classes of nuclear physics experiments, which cannot be done elsewhere.

At ELI-NP the studies that will benefit from high power laser system pulses will focus on laser driven nuclear physics (LDNP). The scientific case of the LDNP TDR encompasses studies of laser induced nuclear reactions, aiming for a better understanding of nuclear properties, of nuclear reaction rates in laser-plasmas, as well as on the development of radiation source characterization methods based on nuclear techniques. An example of the proposed studies: the attempt to achieve solid-state density bunches of (very) heavy ions accelerated to ~10 MeV/nucleon through the RPA mechanism which will be exploited to produce highly astrophysical relevant neutron rich nuclei around the $N \sim 126$ waiting point, using the sequential fission-fusion scheme, complementary to any other existing or planned method of producing radioactive nuclei. Radiation sources of electrons, high energy gammas and protons will be used for specific applications in a number of scientific domains like space science, accelerators and materials studies, medical applications and biology.

The high brilliance gamma beam system of ELI-NP will produce tunable, intense gamma-ray beams with high spectral density, narrow bandwidth, and a high degree of polarization starting in 2017. A rich and versatile program is being prepared for the ELI-NP facility. After commissioning in 2018, it will begin to deliver nuclear structure information from NRF experiments, data from direct measurements of photonuclear reactions, studies of nuclear collective excitations, investigations of the fission-barrier landscape and of mass, charge and angular distributions of fission fragments, as well as spectroscopic and structure studies of neutron-rich nuclei produced in photo fission. Astrophysics and industrial and medical applications are fields that will be advanced by the research at ELI-NP.

Benefiting from the support of a growing international future user community across the globe, the ELI-NP facility is therefore on track with the definition of its science program through the completion of the Technical Design Reports presented in this review paper which allows for the start of the construction of the tools needed for day one experiments in late 2018.

Acknowledgments

We would like to thank the members of the ELI-NP team as well as all our colleagues from all over the world for their contribution to the emerging scientific program of ELI-NP facility and for their tremendous work in implementing the project. This work is supported by the Project Extreme Light Infrastructure—Nuclear Physics (ELI-NP) - Phase I, a project co-financed by the Romanian Government and European Union through the European Regional Development Fund.

References

[1] Mourou G A *et al* (ed) 2011 *ELI—Extreme Light Infrastructure Science and Technology with Ultra-Intense Lasers White book* (Berlin: THOSS Media)
[2] The ELI-NP working groups 2010 The white book of eli nuclear physics www.eli-np.ro/documents/ELI-NP-WhiteBook.pdf
[3] Zamfir N V *et al* 2014 *EPJ Web of Conf.* 6611043
[4] Gales S 2015 *JPS Conf. Proceeding* **6** 020043
[5] Ursescu D *et al* 2014 *The Review of Laser Engineering* **42** 123–6
[6] Balabanski D *et al* 2014 *Acta Phys. Pol.* B **45** 483

[7] Ur C A *et al* 2015 *Nucl. Instr. Meth.* B **355** 198–202
[8] Hajima R *et al* 2008 *J. Nucl. Sci. Tech.* **45** 441–51
[9] Habs D and Koster U 2011 *Appl. Phys.* B **103** 501–19
[10] Hugenschmidt C *et al* 2012 *Appl. Phys.* B **106** 241–9
[11] 2016 ELI-NP Technical Design Reports *Rom. Rep. Phys.* **68**
[12] Yanovsky V *et al* 2008 *Opt. Express* **16** 2109–14
[13] Quesnel B and Mora P 1998 *Phys. Rev.* E **58** 3719
[14] Salamin Y I and Keitel C H 2002 *Phys. Rev. Lett.* **88** 095005
[15] Eliezer S 2002 *The Interaction of High-Power Lasers with Plasmas* ed J Navas (Bristol: IOP Publishing Ltd)
[16] Strickland D and Mourou G 1985 *Opt. Commun.* **56** 219
[17] Robinson A P L, Kwon D H and Lancaster K 2009 *Plasma Phys. Control. Fusion* **51** 095006
[18] Henig A *et al* 2009 *Phys. Rev. Lett.* **103** 245003
[19] Wilks S C *et al* 2001 *Phys. Plasmas* **8** 542
[20] Habs D *et al* 2011 *Appl. Phys.* B **103** 471
[21] Winkler M *et al* 2008 *Nucl. Instrum. Meth. Phys. Res.* B **266** 4183
[22] Gales S 2007 *Prog. Part. Nucl. Phys.* **59** 22–31
[23] Kishimoto S *et al* 2000 *Phys. Rev. Lett.* **85** 1831
[24] Ahmad I *et al* 2000 *Phys. Rev.* C **61** 051304
[25] Kishimoto S *et al* 2005 *Nucl. Phys.* A **748** 3
[26] Gosselin G, Méot V and Morel P 2007 *Phys. Rev.* C **76** 044611
[27] Gobet F *et al* 2011 *Nucl. Instrum. Meth.* A **653** 80
[28] Toncian T *et al* 2006 *Science* **312** 410
Toncian T *et al* 2011 *AIP Advances* **1** 022142
[29] Moustaizis S D *et al* 2001 *AIP Conf. Proc.* **1462** 191–4
[30] Coc A *et al* 1999 *Phys. Rev.* C **61** 015801
[31] Roth M *et al* 2013 *Phys. Rev. Lett.* **110** 044802
[32] Hegelich B M *et al* 2013 *New J. Phys.* **15** 085015
[33] Negoita F *et al* 2016 Laser driven nuclear physics at ELI-NP *Rom. Rep. Phys.* **68**
[34] Pomerantz I *et al* 2014 *Phys. Rev. Lett.* **113** 184801
[35] Martinez M *et al* 2005 *Proc. SPIE* 599159911N
[36] Vartsky D *et al* 2010 *Nucl. Instr. Meth.* A **623** 603
[37] Corde S *et al* 2013 *Rev. Mod. Phys.* **85** 1
[38] Turcu E *et al* 2016 High-field physics and QED experiments at ELI-NP *Rom. Rep. Phys.* **68**
[39] Kim H T *et al* 2013 *Phys. Rev. Lett.* **111** 165002
[40] Leemans W P *et al* 2014 *Phys. Rev. Lett.* **113** 245002
[41] Thomas A G R *et al* 2012 *Physical Review* X **2** 041004
[42] Cipiccia S *et al* 2011 *Nat. Phys.* **7** 867
[43] Nakamura T *et al* 2012 *Phys. Rev. Lett.* **108** 195001
[44] Tesileanu O *et al* 2016 Combined laser gamma experiments at ELI-NP *Rom. Rep. Phys.* **68**
[45] Rossi L 2011 *LHC Upgrade Options and Plans Proc. of IPAC2* (Spain: San Sebastian) 011 HL-LHC website urlhttp://cern.ch/HiLumiLHC
[46] Adriani O *et al* 2014 *Technical Design Report EuroGammaS proposal for the ELI-NP Gamma beam System* arXiv:1407.3669v1 [physics.acc-ph]
[47] Bacci A *et al* 2013 *J. App. Phys.* **113** 194508
[48] Ferrario M *et al* 2010 *Phys. Rev. Lett.* **104** 054801
[49] Alesini D *et al* 2015 *Phys. Rev. STAB.* **18** 092001
[50] Federici L *et al* 1980 *Nuovo Cimento Lett* **27** 339
[51] Federici L *et al* 1980 *Nuovo Cimento* B **59** 247
[52] Sandorfi A M *et al* 1984 *IEEE. Trans.* **NS-30** 3083
[53] Litvinenko V N *et al* 1997 *Phys. Rev. Lett.* **78** 4569
[54] Babusci D *et al* 1990 *Nuovo Cimento* A **103** 1555
[55] Kezerashvili G Y *et al* 1993 *Nucl. Instrum. Meth.* A **328** 506
[56] Kezerashvili G Y *et al* 1998 *Nucl. Instrum. Meth.* B **145** 40
[57] Nakano T *et al* 1998 *Nucl. Phys.* A **629** 559c
[58] Nakano T *et al* 2001 *Nucl. Phys.* A **684** 71c
[59] Amano S *et al* 2009 *Nucl. Instrum. Meth. Phys. Res.* A **602** 337
[60] Toyokawa H *et al* 2009 *It Nucl. Instrum. Meth. Phys. Res.* A **608** S41–3
[61] Dupraz K *et al* 2014 *Phys. Rev. STAB.* **17** 033501
[62] Cardarelli P *et al* 2015 *Nucl. Instr. Meth.* **B355** 237
[63] Moon P B 1951 *Proc. Phys. Soc.* A **64** 76
[64] Bohle D *et al* 1984 *Phys. Lett.* B **137** 27
[65] Lipas P O 1966 *Nucl. Phys.* **82** 91
[66] Donner W and Greiner W 1966 *Z. Phys.* **197** 440
[67] Ohgaki H *et al* 1994 *Nucl. Instr. Meth. Phys. Res.* A **353** 384
[68] Weller H R *et al* 2009 *Prog. Part. Nucl. Phys.* **62** 257
[69] Löher B *et al* 2013 *Nucl. Instr. Meth. Phys. Res.* A **723** 136
[70] Pietralla N *et al* 2002 *Phys. Rev.* C **65** 047305
[71] Fransen C *et al* 2004 *Phys. Rev.* C **70** 044317
[72] Savran D *et al* 2005 *Phys. Rev.* C **71** 034304
[73] Pietralla N *et al* 2009 *Phys. Lett.* B **681** 134
[74] Tonchev A P *et al* 2010 *Phys. Rev. Lett.* **104** 072501
[75] Beller J *et al* 2015 *Phys. Lett.* B **741** 128
[76] Ur C A *et al* 2016 Nuclear resonance fluorescence experiments at ELI-NP *Rom. Rep. Phys.* **68**
[77] Suliman G *et al* 2016 Gamma—beam industrial applications at ELI-NP *Rom. Rep. Phys.* in press
[78] Brink D 1955 *PhD Thesis* Oxford University
[79] Axel P 1962 *Phys. Rev.* **126** 671
[80] Baran V *et al* 2013 *Phys. Rev.* C **88** 044610
[81] Brown B A and Schwenk A 2014 *Phys. Rev.* C **89** 011307
[82] Metzger R R 1959 *Prog. Nucl. Phys.* **7** 54
[83] Pietralla N *et al* 1995 *Phys. Rev.* C **51** 1021
[84] Romig C *et al* 2015 *Phys. Lett.* B **744** 369
[85] Guttormsen M *et al* 2012 *Phy. Rev. Lett* **109** 162503
[86] Svensson C E *et al* 2005 *Nucl. Instr. Meth. Phys. Res.* A **540** 348
[87] Daito I *et al* 2016 *Energy Precedia* **89** 389–94
[88] Hagmann C A *et al* 2009 *J. of Appl. Phys.* **106** 084901
[89] Beck O *et al* 1998 *J. of Appl. Phys.* **83** 5484
[90] Balabanski D L *et al* 2016 GBS-tdr3 photofission experiments at ELI-NP *Rom. Rep. Phys.* **68**
[91] Balabanski D L 2015 *Pramana* **85** 473–81
[92] Balabanski D L 2015 *Bulg. J. Phys.* **42** 372–81
[93] Thirolf P G and Habs D 2002 Prog *Prog. Nucl. Part. Phys.* **49** 352
[94] Krasznahorkay A 2011 (Handbook of Nuclear Chemistry vol 1) ed A Vertes *et al* (New York: Springer) 281
[95] Thirolf P G *et al* 2012 *EPJ Web of Conf.* **38** 061302
[96] Polikanov *et al* 1962 *Soviet. Phys. JETP* **15** 1016
[97] Strutinsky V M 1967 *Nucl. Phys.* A **95** 420
[98] Back B B *et al* 1972 *Phys. Rev. Lett.* **28** 1707
[99] Moller P, Nilsson S G and Sheline R K 1972 *Phys. Lett.* B **40** 329
[100] Cwiok S *et al* 1994 *Phys. Lett.* B **322** 304
[101] Jachimowicz P, Kowal M and Skalski J 2013 *Phys. Rev.* C **85** 044308
[102] Kowal M and Skalski J 2012 *Phys. Rev.* C **85** 061302
[103] Back B B *et al* 1974 *Phys. Rev.* C **9** 1924
[104] Bellia G *et al* 1983 *Z. Phys.* A **314** 43
[105] Bowman C D *et al* 1978 *Phys. Rev.* C **17** 1086
[106] Dickey P A and Axel P 1975 *Phys. Rev. Lett.* **35** 501
[107] Knowles J W *et al* 1982 *Phys. Lett.* **116B** 315
[108] Zhuchko V E, Ostapenko Yu B, Smirenkin G N, Soldatov A S and Tsypenyuk Yu M 1978 *Yad. Fiz.* **28** 1185
[109] Ostapenko Yu B, Smirenkin G N, Soldatov A S and Tsypenyuk Yu M 1981 *Phys. Rev.* C **24** 529
[110] Csige L *et al* 2013 *Phys. Rev.* C **87** 044321
[111] Shalem C K *et al* 2006 *Nucl. Instr. Meth.* A **258** 468
[112] Budtz-Jorgensen C *et al* 1987 *Nucl. Instr. Meth.* A **258** 209
[113] Neubert W 1985 *Nucl. Instr. Meth.* A **237** 535
[114] Van Duppen P 2006 *Lect. Notes. Phys.* **700** 37–77
[115] Morrissey D J and Sherill B M 2004 *Lect. Notes. Phys.* **651** 113–35
[116] Essaba E *et al* 2003 *Nucl. Instrum. Meth. Phys. Res.* B **204** 780–4
[117] Dilling J, Krücken R and Merminga L (ed) 2014 *ISAC and ARIEL: The TRIUMF Radioactive Beam Facilities and the Scientific Program* (Netherlands: Springer)

[118] Aysto Y *et al* 2014 *Three decades of research using igisol at the University of Jyvaskyla* (Netherlands: Springer)
[119] Bollen G 2004 *Lect. Notes. Phys.* **651** 169–210
[120] Schwarz S *et al* 2003 *Nucl. Instr. Meth.* B **204** 507
[121] Wada M *et al* 2003 *Nucl. Instr. Meth.* B **204** 570
[122] Savard G *et al* 2003 *Nucl. Instr. Meth.* B **204** 582
[123] Plass W *et al* 2013 *Nucl. Instr. Meth.* B **317** 457
[124] Balabanski D L *et al* 2016 *Rom. Rep. Phys.* in print
[125] Constantin P, Balabanski D L and Cuong P V 2016 *Nucl. Instr. Meth.* B **372** 78–85
[126] Cadwell J T *et al* 1980 *Phys. Rev.* C **21** 1215
[127] Csige L *et al* 2013 *Phys. Rev.* C **87** 044321
[128] Cuong P V 2009 *PhD Thesis* University Paris XI, Orsay
[129] Donzaud C *et al* 1998 *Eur. Phys. J.* A **1** 407
[130] Constantin P, Balabanski D L and Cuong P V 2016 *Nucl. Instr. Meth.* B submitted
[131] Bothe W and Gentner W 1937 *Z. Phys.* **71** 236
[132] Migdal A B 1944 *J. Phys. (USSR)* **8** 331
[133] Baldwin G C and Klaiber G 1947 *Phys. Rev.* **71** 3
[134] Goldhaber M and Teller E 1948 *Phys. Rev.* **74** 1046
[135] Paar N, Vretenar D, Khan E and Colò G 2007 *Rep. Prog. Phys.* **70** 691
[136] Carbone A *et al* 2010 *Phys. Rev.* C **81** 041301
[137] Wieland O *et al* 2006 *Phys. Rev. Lett.* **97** 012501
[138] Shiller A and Thoennessen M 2007 *At. Data Nucl. Data Tables* **93** 549
[139] Adrich P *et al* 2005 *Phys. Rev. Lett.* **95** 132501
[140] Utsunomiya H *et al* 2010 *Phys. Rev.* C **81** 035801
Utsunomiya H *et al* 2010 *Phys. Rev.* C **82** 064610
[141] Heckman P *et al* 2003 *Phys. Lett.* **B555** 43–8
[142] Tamii A *et al* 2011 *Phys. Rev. Lett.* **107** 062502
[143] Savran D *et al* 2006 *Phys. Rev. Lett.* **97** 172502
[144] Savran D *et al* 2008 *Phys. Rev. Lett.* **100** 232501
[145] Iwamoto C, Utsunomiya H, Tamii A *et al* 2012 *Phys. Rev. Lett.* **108** 262501
[146] Filipescu D *et al* 2015 *Eur. Phys. J.* A **51** 185
[147] Camera F *et al* 2016 *Rom. Rep. Phys.* **68**
[148] Filipescu D *et al* 2016 GBS-TDR2 gamma above the neutron threshold experiments at ELI-NP *Rom. Rep. Phys.* in print
[149] Fowler W A 1984 *Rev. Mod. Phys.* **56** 149
[150] Kunz R *et al* 2001 *Phys. Rev. Lett.* **86** 3244
[151] Hammer J W *et al* 2005 *Nucl. Phys.* A **752** 514c
[152] Hammer J W *et al* 2005 *Nucl. Phys.* A **758** 363c
[153] Assuncao M *et al* 2006 *Phys. Rev.* C **73** 055801
[154] Plag R *et al* 2012 *Phys. Rev.* C **86** 015805
[155] Thielemann F-K *et al* 2004 *New Astro. Rev.* **48** 605
[156] Perlmutter S 2012 *Mod. Phys. Rev.* **84** 1127
Schmidt B P 2012 *Mod. Phys. Rev.* **84** 1151
Riess A G 2012 *Mod. Phys. Rev.* **84** 1165
[157] Schuermann D *et al* 2011 *Phys. Lett.* B **703** 557
[158] Dababneh S *et al* 2003 *Phys. Rev.* C **68** 025801
[159] Wiescher M *et al* 1980 *Nucl. Phys.* A **349** 165
[160] Angulo C *et al* 1999 *Nucl. Phys.* A **656** 3
[161] Buckner M Q *et al* 2012 *Phys. Rev.* C **86** 065804
[162] Gai M *et al* 2010 *JINST* **5** 12004
[163] Pollacco E *et al* 2012 *Physics Procedia* **37** 1799
[164] Sauli F 2007 *NIM* A **580** 971
[165] Sauli F 1998 *NIM* A **189** 419
[166] Matos M *et al* 2011 *PoS (NIC XI)* 226 p
[167] Nyhus H T *et al* 2015 *Phys. Rev.* C **91** 015808
[168] Azaiez F *et al* (ed) 2014 *Nuclear Physics for Medicine NuPPeC Report* European Science Foundation http://nupecc.org/pub/npmed2014.pdf
[169] Ice R D 1995 *Health Phys.* **69** 721–7
[170] Habs D *et al* 2011 *Proc. SPIE* **8079** 80791H
[171] Qaim S M 2012 *Radiochim. Acta* **100** 635–51
[172] Bobeica M *et al* 2016 GBS-TDR5.3 radioisotope production for medical applications at ELI-NP *Rom. Rep. Phys.* **68**
[173] Luo W *et al* 2016 *Appl. Phys.* B **122** 8
[174] Carroll J J *et al* 1991 *Phys. Rev.* C **43** 1238
[175] Shizuma T *et al* 2005 *Phys. Rev.* C **72** 025808